

**KWAME NKRUMAH UNIVERSITY OF SCIENCE AND
TECHNOLOGY, KUMASI**

**SYNTHESIS, DERIVATIZATION, CHARACTERIZATION AND
ANTI-MICROBIAL SCREENING OF AZO COMPOUNDS.**

BY

KWAKU ADDO-DANQUAH

**DISSERTATION SUBMITTED TO THE DEPARTMENT OF
PHARMACEUTICAL CHEMISTRY OF THE FACULTY OF
PHARMACY AND PHARMACEUTICAL SCIENCES KNUST, IN
PARTIAL FULFILMENT OF THE REQUIREMENTS FOR THE
AWARD OF MASTER OF PHILOSOPHY DEGREE IN
PHARMACEUTICAL CHEMISTRY**

MAY, 2016

DECLARATION

I hereby declare that this thesis report is my own work and that the work was undertaken at the Department of Pharmaceutical Chemistry. To the best of my knowledge, it has not been submitted for the award of any degree or certificate from any institution, except where due acknowledgement has been made in the text.

| | | |
|---------------------|-------------|--------|
| KWAKU ADDO-DANQUAH | | |
| (PG 2749214) | | |
| (Name of candidate) | (Signature) | (Date) |

| | | |
|-------------------|-------------|--------|
| DR. WILLIAM KOFIE | | |
| (Main Supervisor) | (Signature) | (Date) |

| | | |
|-------------------------------------|-------------|--------|
| DR. MRS ABENA AMPONSAA BROBBEY..... | | |
| (Auxiliary Supervisor) | (Signature) | (Date) |

| | | |
|----------------------|-------------|--------|
| DR. ISAAC AYENSU | | |
| (Head of Department) | (Signature) | (Date) |

DEDICATION

This work is dedicated to my sister, Ama Anima Addo-Danquah.

ACKNOWLEDGEMENT

“If I have been able to see further, it is by standing on the shoulders of giants”

– Sir Isaac Newton

First and foremost, I thank the Almighty Father for the strength and grace throughout this program.

To my supervisors, Dr. William Kofie and Dr. Mrs. Abena Amponsaa Brobbey, I want to say a big thank you for your support, guidance, motivation and insight in directing this research work. God richly bless you.

I would also like to thank members of the Synthesis group, my course mates and all members of staff at the Department of Pharmaceutical Chemistry for their help.

Special thanks goes to my family, for their love, encouragement, prayers and financial support to make this dream a reality. I love you all.

Finally, am grateful for the help of my friends, Philip Kpe, James Gyimah Manu, Stephen Opoku Damoah, Naomi Agyei and Emmanuella Adjei-Sowah for being there when times were tough. Thanks guys.

ABSTRACT

In our research group, two *azo* dyes were recently demonstrated to have antimicrobial activity. Structural modification of these compounds resulted in seven novel dyes. Five compounds were synthesised by the two-step diazotization-coupling reaction sequence. Employing the Williamson's synthesis and acetylation with acetic anhydride, the ether and acetyl derivatives were synthesised respectively. The synthesised dyes, with good yields, have been characterised with IR, Mass Spec. and ¹H NMR, and the melting point as well as retardation factor determined. The Broth Dilution method was used in determining the antimicrobial activity against the organisms, *Staphylococcus aureus*, *Streptococcus pyrogenes*, *Salmonella typhi*, *Pseudomonas aeruginosa* and *Candida albicans*. The synthesised compounds showed a broad spectrum of activity, with greater gram-negative and antifungal activity. The alkylated products, (E)-1-(4-ethoxynaphthalen-1-yl)-2-(4-nitrophenyl)diazene (KA 008), (E)-4-((4-ethoxynaphthalen-1-yl)diazanyl benzoic acid (KA 009) were the most active of all the compounds synthesised, with an MIC of 35.16µg/ml against *P. aeruginosa* and *S. pyrogenes* for KA 008 and 70.32 µg/ml against *S. typhi* and *P. aeruginosa* for KA 009. The acetylated derivatives showed the least activity against the test organisms. KA 008 also showed comparable activity against the standard Cefuroxime axetil used as the positive control.

TABLE OF CONTENTS

| | |
|--|------|
| DECLARATION | i |
| DEDICATION | ii |
| ACKNOWLEDGEMENT | iii |
| ABSTRACT..... | iv |
| TABLE OF CONTENTS..... | v |
| LIST OF FIGURES | viii |
| LIST OF SCHEMES..... | x |
| LIST OF TABLES | xi |
| LIST OF ABBREVIATIONS | xi |
| CHAPTER ONE | 1 |
| INTRODUCTION | 1 |
| 1.1 BACKGROUND OF STUDY | 1 |
| 1.1.1 History of antimicrobials | 1 |
| 1.1.2 Diazo Compounds..... | 2 |
| 1.2 PROBLEM STATEMENT | 3 |
| 1.3 OBJECTIVES | 6 |
| 1.3.1 General objective | 6 |
| 1.3.2 Specific Objectives | 6 |
| CHAPTER TWO | 7 |
| LITERATURE REVIEW | 7 |
| 2.1 HISTORY OF ANTIMICROBIAL DRUGS | 7 |
| 2.2 DYESTUFFS | 9 |
| 2.3 AZO DYES | 11 |
| 2.4 AZO COMPOUNDS | 12 |

| | | |
|-------|--|----|
| 2.4.1 | Origin | 13 |
| 2.4.2 | General Mechanism | 13 |
| 2.5 | BIOLOGICAL ACTIVITY OF AZO COMPOUNDS..... | 14 |
| 2.5.1 | Antiviral Activity | 16 |
| 2.5.2 | Anti-microbial activity of <i>azo</i> -containing Schiff bases | 16 |
| 2.5.3 | Anti-microbial activity of <i>azo</i> -containing heterocycles..... | 18 |
| 2.5.4 | Anti-microbial activity of naphthol <i>azo</i> dyes..... | 21 |
| | CHAPTER THREE | 24 |
| | MATERIALS AND METHODS..... | 24 |
| 3.1 | MATERIALS | 24 |
| 3.1.1 | Reagents | 24 |
| 3.1.2 | Equipment and Instrument..... | 25 |
| 3.2 | METHODS..... | 25 |
| 3.2.1 | General procedure for the formation of the diazonium salt..... | 25 |
| 3.2.2 | General procedure for the coupling reaction | 26 |
| 3.2.3 | Procedure for formation of the acetylated products..... | 31 |
| 3.2.4 | Procedure for the formation of the alkylated products | 33 |
| 3.2.5 | Antimicrobial Assay | 35 |
| | CHAPTER FOUR..... | 36 |
| | RESULTS | 36 |
| 4.1 | SYNTHESIS | 36 |
| 4.2 | ANTIMICROBIAL ASSAY..... | 38 |
| | CHAPTER FIVE | 39 |
| | DISCUSSIONS, CONCLUSION AND RECOMMENDATIONS..... | 39 |
| 5.1 | DISCUSSION | 39 |

| | | |
|-------|---------------------------|----|
| 5.1.1 | Synthesis | 39 |
| 5.1.2 | Spectral Analysis | 43 |
| 5.1.3 | Antimicrobial Assay | 56 |
| 5.2 | CONCLUSION | 60 |
| 5.3 | RECOMMENDATION | 61 |
| | REFERENCES | 62 |
| | APPENDICES | 67 |

LIST OF FIGURES

| | |
|--|----|
| Figure 1.1 Structure of prontosil (a) and balsalazide (b) | 3 |
| Figure 1.2 Structure of p-ABA α N (a) and p-NA α N (b) | 5 |
| Figure 2.1 Structure of Salvarsan..... | 7 |
| Figure 2.2 Structures of some early dyes..... | 10 |
| Figure 2.3 Structure of Mauveine | 11 |
| Figure 2.4 Structures of the first synthesised azo dyes | 12 |
| Figure 2.5 Structure of benzidine..... | 14 |
| Figure 2.6 Structure of Direct Black 38..... | 15 |
| Figure 2.7 Structure of PEG immobilised on a dye..... | 15 |
| Figure 2.8 Structure of FP-21399 | 16 |
| Figure 2.9 Structure of Schiff base ligand and metal complex..... | 18 |
| Figure 2.10 Structure of thiadiazole and diazonium salt derivative | 19 |
| Figure 2.11 Structure of 8-hydroxy quinolone coupled thiazole derivative | 20 |
| Figure 2.12 Structure of benzothiazole..... | 20 |
| Figure 2.13 Structure of the benzothiazole coupled methoxy amide derivative | 21 |
| Figure 2.14 Structure of p-ABA α N (a) and p-NA α N (b) | 22 |
| Figure 5.1 Structure of p-ABA α N (a) and p-NA α N (b) | 39 |
| Figure 5.2 Molecular ion in a) positive and b) negative ionization modes..... | 45 |
| Figure 5.3 Fragment (ion) with m/z of 126.0 (a) and 246 (b)..... | 46 |
| Figure 5.4 Fragment (ion) with m/z of 292.3..... | 48 |
| Figure 5.5 Fragment (ion) with m/z of (a) 246.3 and (b) 177.2..... | 49 |
| Figure 5.6 Fragment with m/z of 280.0 | 51 |
| Figure 5.7 Fragment (ion) with m/z of (a) 183.9 and (b) 169.9..... | 51 |

| | |
|--|----|
| Figure 5.8 Fragment (ion) with m/z of 144.8 (a) and 137.0 (b)..... | 52 |
| Figure 5.9 Molecular ion formed in positive (a) and negative (b) modes | 54 |
| Figure 5.10 Fragments with m/z of 139.0 (a) and 170.0 (b)..... | 54 |
| Figure 5.11 Structures of the most active synthesised dyes..... | 61 |

LIST OF SCHEMES

| | |
|---|----|
| Scheme 2.1 Reduction of Prontosil by azo reductase enzyme..... | 8 |
| Scheme 2.2 Diazotization of Picramic acid by Griess | 13 |
| Scheme 2.3 General reaction pathway for the formation of azo dyes | 14 |
| Scheme 5.1 General reaction pathway for the formation of azo dyes | 40 |
| Scheme 5.2 General scheme for the synthesis of the acetylated products..... | 41 |
| Scheme 5.3 General scheme for the synthesis of the alkylated products | 42 |

LIST OF TABLES

| | |
|--|----|
| Table 3.1 Reagents and materials used with their sources..... | 24 |
| Table 4.1 Synthesised azo compounds with their physical data | 36 |
| Table 4.2 Minimum Inhibition Concentrations (MIC) of the synthesised dyes | 38 |

LIST OF ABBREVIATIONS

| | |
|----------------------|---|
| AMR – | Antimicrobial resistance |
| Ar – | Aromatic |
| ATCC – | American Type Culture Collection |
| CDC – | Center for Disease Control |
| CD4 – | Cluster Differentiation 4 cell |
| d – | Doublet |
| DMAP – | Dimethylaminopyridine |
| ES – | Electrospray (positive or negative mode) |
| eq – | equivalent |
| ¹ H NMR – | Proton Nuclear Magnetic Resonance |
| HIV – | Human Immunodeficiency Virus |
| Hz – | Hertz |
| IR – | Infra-Red Spectroscopy |
| IUPAC – | International Union of Pure and Applied Chemistry |
| m – | Multiplet |
| LCD – | Liquid Crystal Display |
| M ⁺ – | Molecular ion |
| m/z – | mass-to-charge ratio |
| MDR – | Multidrug resistance |
| MDR-TB – | Multidrug-resistant tuberculosis |
| MHz- | Mega Hertz |
| MIC – | Minimum inhibitory concentration |
| mg – | Milligrams |
| MS – | Mass Spectrometry |
| NLO – | Nonlinear Optical |
| nm – | Nanometers |
| °C – | degrees Celsius |
| PDT – | Photodynamic Therapy |
| PEG – | Polyethylene glycol |

| | |
|----------|-----------------------------------|
| ppm – | Parts per million |
| Rf – | Retardation factor |
| s – | Singlet |
| TLC – | Thin Layer Chromatography |
| µg – | Micrograms |
| µL – | Microliters |
| δ – | Chemical shift |
| UV-Vis – | Ultra Violet-Visible Spectroscopy |
| WHO – | World Health Organisation |

CHAPTER ONE

INTRODUCTION

1.1 BACKGROUND OF STUDY

1.1.1 History of antimicrobials

Antimicrobial medicines are agents designed to destroy or inhibit the growth of organisms including bacteria, viruses and parasites. However, in recent times, resistance to commonly administered antimicrobial agents by these organisms is a common occurrence. Organisms that have developed resistance are able to withstand the destruction that otherwise the medicine would have caused. This renders the medicine ineffective and the infections may persist and spread to others (Neu, 1992).

Over the last decade, there has been an increase in the number and proportion of bacterial that has grown resistant to commonly administered anti-bacterial agents, leading to the development of multidrug resistance (MDR) bacteria. This has led to organizations such as the United States' Centre for Disease Control (CDC), the European Centre for Disease Prevention and Control (ECDC) and the World Health Organization (WHO) to label infections caused by MDR bacteria as an emergent global health epidemic (Roca *et al.*, 2015).

Responding to the increasing threat posed by antimicrobial resistance (AMR) and MDR, WHO proposed some measures which they believe can help curtail the situation. The measures are;

- bringing all stakeholders together to agree on and work towards a coordinated response;

- strengthening national stewardship and plans to tackle antimicrobial resistance;
- generating policy guidance and providing technical support for Member States;
- actively encouraging innovation, research and development.

The development of fluoroquinolones as antibiotic agents happened about 40 years ago. After fluoroquinolones, there has been limited development of major antibiotic agents. As a result, a gap has been created between the occurrence of new infections and new agents to fight them (WHO, 2014).

1.1.2 Diazo Compounds

Aromatic diazo compounds, containing the functional group Ar-N=N-Ar , form the largest class of dyes in use today. Their extensive conjugation, affording them varying shades of colours, contribute to their use as dyes (Rasheed, 2011).

Interest in diazo compounds, however, is not limited only to their use as dyes, but also their medicinal application. Commercially available medicines containing diazo functionality include; Prontosil, which is used as an antibacterial agent (Wainwright and Kristiansen, 2011) and Balsalazide, used to treat inflammatory bowel disease (Tursi *et al.*, 2004) (fig. 1.1).

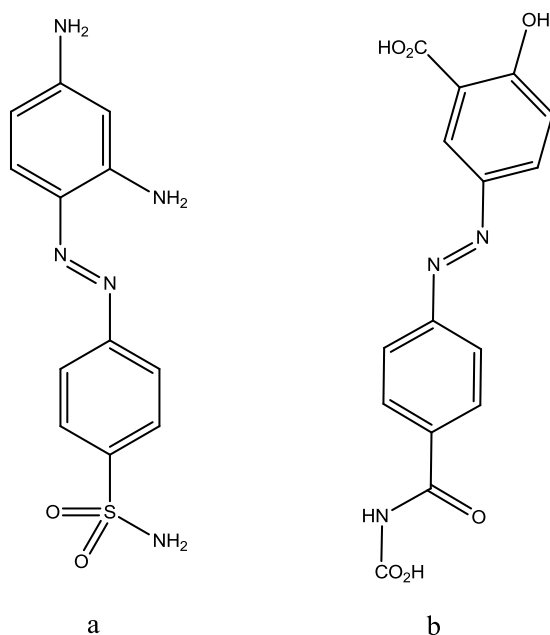


Figure 1.1 Structure of prontosil (a) and balsalazide (b)

Recent research has revealed that some synthetic diazo compounds possess antimicrobial activity (Avcı *et al.*, 2012, Hayashi *et al.*, 2001, Kofie *et al.*, 2015, Shridhar *et al.*, 2011).

1.2 PROBLEM STATEMENT

In 2014, WHO reported that the problem with antimicrobial resistance is no longer a prediction for the future, but it is now a common occurrence. This is threatening the health provision by making common infections difficult to treat. Treatment for common infections and minor injuries are becoming ineffective and death from such conditions would become common occurrence again. This is leading the world towards a post-antibiotic era. For instance, in several countries, there have been reports of the failure of third generation cephalosporins in treating gonorrhoea. Widespread resistance to fluoroquinolones by *E. coli* as well as resistance to first-line drugs in the treatment of infections by *Staphylococcus aureus* has been reported. The

incident of multidrug-resistant tuberculosis (MDR-TB) is on the increase worldwide (WHO, 2014, Lowy, 2003).

The phenomenon of the development of resistance to antimicrobial drugs by microorganisms is natural. However, the inappropriate use of these drugs has contributed greatly in the resistance process. Another source for the increasing prevalence of resistance is the lack of new antimicrobial agents to tackle new infections. After the fluoroquinolones were discovered, there has not been the development of a major antimicrobial drug in the past few decades. The WHO recommends that the problem with resistance can be addressed and curtailed through the act of collaborative effort between policy makers and researchers, among other recommendations, to develop new vaccines (WHO, 2014, Roca *et al.*, 2015).

In light of these recommendations, seven *azo* compounds were recently synthesised by our research group and their antimicrobial activity determined. Of the compounds synthesised, two demonstrated encouraging antimicrobial potentials (fig 1.2). The two compounds are (E)-4-((4-hydroxynaphthalen-1-yl) diazenyl) benzoic acid, code-named *p*-ABA α N, and (E)-4-((4-nitrophenyl) diazenyl) naphthalen-1-ol, code-named *p*-NA α N.

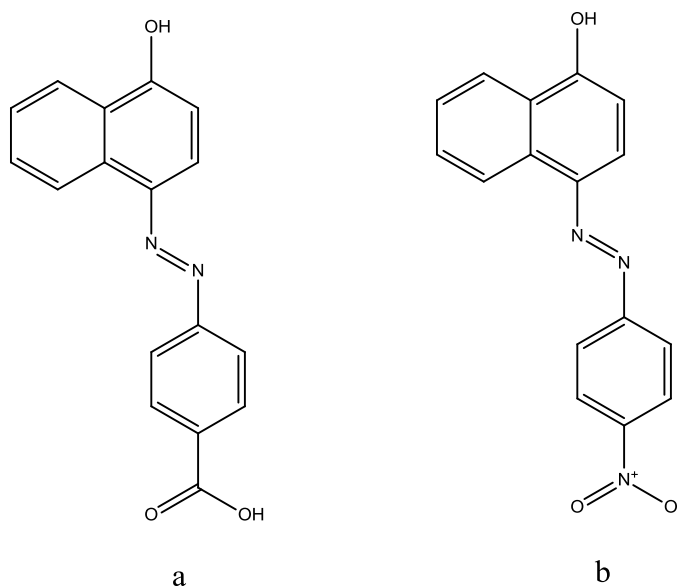


Figure 1.2 Structure of *p*-ABA α N (a) and *p*-NA α N (b)

p-ABA α N showed inhibition against the fungus, *Candida albicans*. *p*-NA α N on the other hand showed a broad spectrum antimicrobial activity against all the test organisms used, recording a low minimum inhibitory concentration (MIC) of 0.02mg/ml against *C. albicans* with the highest of 4.06mg/ml against *Mycobacterium smegmatis* (Kofie *et al.*, 2015).

Considering the structure of the two compounds, the hydroxyl group on the naphthol, the carboxylic acid group as well as the aromatic ring system provides suitable site for the modification of the structure of the compounds. Therefore the formation of derivatives of these two dyes focusing on the carboxylic, phenol and aromatic ring functionalities will be the basis of this present research.

1.3 OBJECTIVES

1.3.1 General objective

The aim of this research involves the synthesis and derivatization of *azo* compounds, *p*-ABA α N and *p*-NA α N and screening for their antimicrobial properties.

1.3.2 Specific Objectives

- To use readily available reagents to synthesise the *azo* compounds and their derivatives employing the standard diazotization and coupling procedure.
- To use spectroscopic methods – Infra-Red, Proton Nuclear Magnetic Resonance and Mass Spectrometry – to characterize the synthesised compounds.
- To determine the physicochemical parameters of the synthesised compounds including melting point and retardation factor (rf).
- To investigate the *in-vitro* antimicrobial activity of the compounds against the microorganisms, *Staphylococcus aureus*, *Streptococcus pyrogenes*, *Salmonella typhi*, *Pseudomonas aeruginosa* and *Candida albicans*.

CHAPTER TWO

LITERATURE REVIEW

2.1 HISTORY OF ANTIMICROBIAL DRUGS

Introduction of antimicrobial drugs meant an end to the deaths associated with infectious diseases, resulting in improved life of the human race. Such was the advances made in the so-called “golden-era” of antimicrobial drug development that it was believed that total eradication of infectious disease would be achieved in the not so long future.

In the year 1910, Paul Ehrlich successfully synthesised a drug that could treat syphilis through the “magic bullet” idea. This idea was grounded on the observation that, aniline and other synthetic dyes, present at the time, could stain only certain microbes. As a result, Ehrlich embarked on the journey of specifically designing a treatment for the *Treponema pallidum* causing disease. He called the new drug *Salvarsan* (fig 2.1) which became the most widely prescribed drug at the time (Wainwright, 2008).

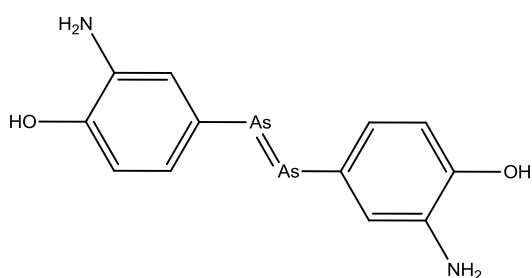
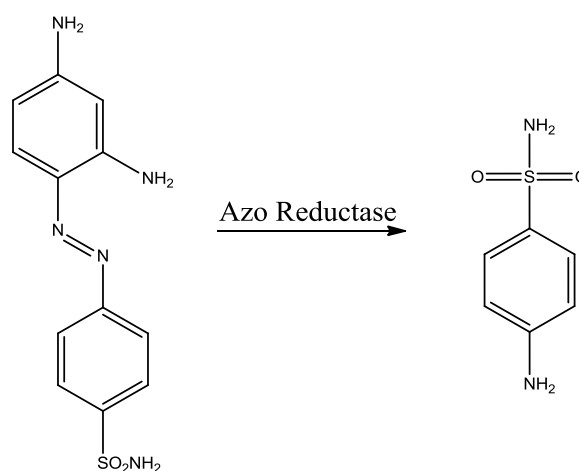


Figure 2.1 Structure of Salvarsan

This was followed by the sulfa drugs, the first of which was synthesised by Mietzsch and Klarer. Gerhard Domagk investigated the antimicrobial activity of the new compound, prontosil. It was revealed later that, prontosil was the precursor of sulphanilamide, (Scheme 2.1) the active part. This kick-started

the development of the sulphonamide group of antibiotics (Wainwright and Kristiansen, 2011).



Scheme 2.1 Reduction of Prontosil by azo reductase enzyme

The serendipitous discovery of penicillin by Alexander Fleming in 1928, led to the saving of the lives of many injured soldiers during the Second World War. It was not until the 1940s before the problem of the purification and stabilization of the active compound was addressed and penicillin entered into mass production (Fleming, 1946). With the discovery of these three classes of antimicrobials, the foundation was laid for other researchers to take up the mantle and develop other drugs. The period between the 1950s and 1970s saw the introduction of new classes of antibiotics, from the cephalosporins through to the carbapenems and to the fluoroquinolones (Andriole, 2005, Bo, 2000, Sykes and Bonner, 1985). After this period, a vacuum has been created in terms of the addition of novel class to treat emerging and re-emerging infections. The focus of most research has been the modification of existing antibiotics in recent time (WHO, 2014).

2.2 DYESTUFFS

A dye can be defined as an organic compound used to give colour to a substrate. The mechanism by which the colour is imparted includes physical adsorption, formation of complexes with metals or salts or mechanical retention. Absorption in the visible region (400-800) of the electromagnetic spectrum, gives dyes their colours. Witt proposed that, the presence of a chromophore and an auxochromes are essential for a dye; the chromophore giving the colour while the auxochromes deepens the colour. This theory has been replaced by the modern electronic theory, which states that the excitation of valence π electrons after the absorption of visible light, results in colour (Bafana *et al.*, 2011).

The use of dyes dates back to ancient times. Egyptian mummies were wrapped in cloth dyed with *Indigo*. It is believed that, Alexander the Great sprinkled on his army, alizarin (a red dye) to deceive the Persian armies into thinking they were injured. The togas of the Roman Emperors was dyed with *Tyrian purple*, a dye obtained for the Murex snails (Garfield, 2002, Morris and Travis, 1992). The structures for *Indigo*, alizarin and *Tyrian purple* are shown in fig. 2.2

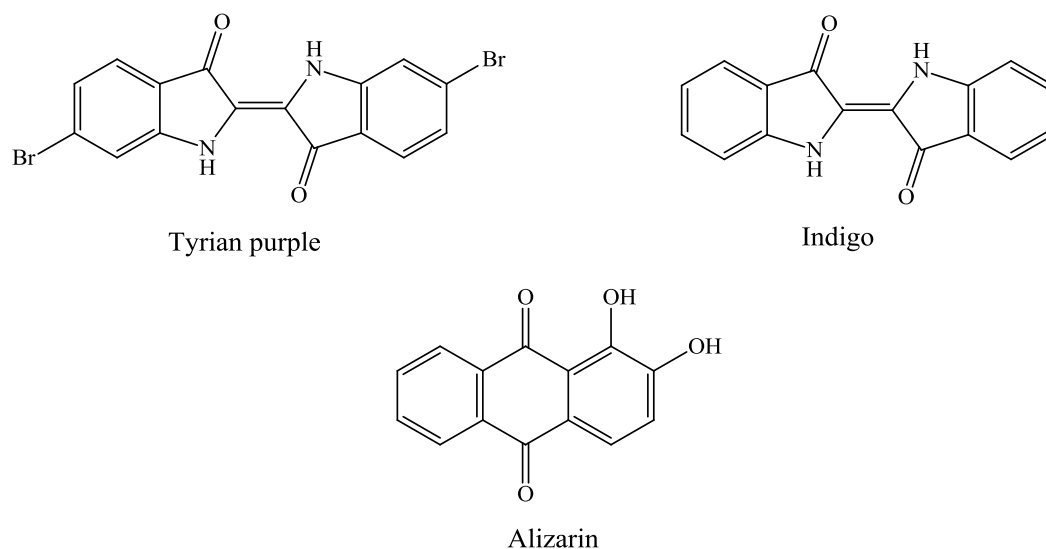


Figure 2.2 Structures of some early dyes

Before the mid-19th century, all the dyes in use were from natural sources, most of which were extracted from vegetables with a few animal sources. The diversity of the colours possessed by these dyes were limited and pushed researchers to develop synthetic dyes with varying colours. With this goal, Woulfe in 1771 developed the yellow coloured picric acid by reacting *Indigo* with nitric acid. The first synthetic dye, *Mauveine* (fig 2.3), however, was developed by William Henry Perkin in 1856. He was trying to synthesise quinine to treat malaria but failed in this quest. However when washing the reaction flask with alcohol, he observed that a purple solution was formed. After this, dozens other synthetic dyes have been developed and are in use to date (Garfield, 2002).

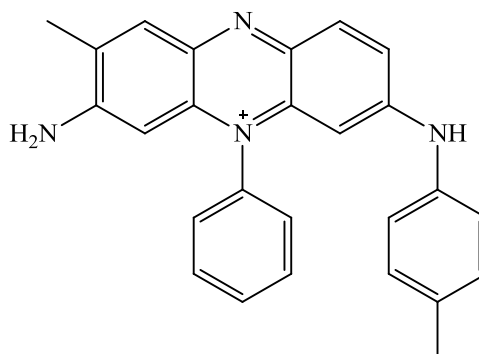


Figure 2.3 Structure of Mauveine

2.3 AZO DYES

Azo dyes make up about 70% of all organic dyes in use currently worldwide. The popularity and widespread use of *azo* dyes is as a result of the relative simple method of synthesis, diverse variety of colours, great structural diversity and medium-to-high fastness properties. They find use in the textile, cosmetic, food, medical, printing and paint industries. *Azo* dyes are also used on the high technology areas like electro-optical devices, liquid crystal displays, lasers and ink-jet printers (Natansohn and Rochon, 2002, Yaroshchuk and Reznikov, 2012, Harada *et al.*, 2005).

Aniline Yellow and Bismarck Brown (fig 2.4) synthesised by Mene in 1861 and Martius in 1863 respectively, are the first *azo* dyes prepared. Structurally, Bismarck Brown contains two *azo* linkages, making it a *bisazo* dye. The presence of the second *azo* helps to extend the conjugation of the dye hence absorbs visible light of longer wavelength than the Aniline Yellow dye.

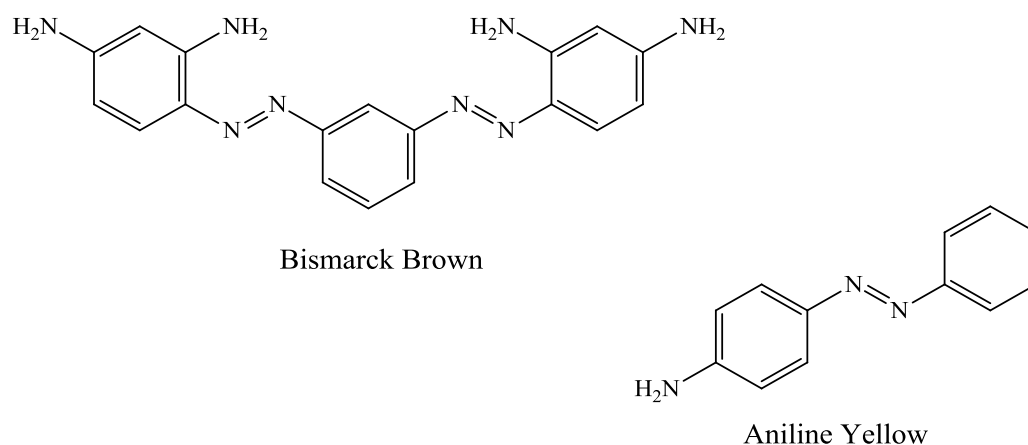


Figure 2.4 Structures of the first synthesised azo dyes

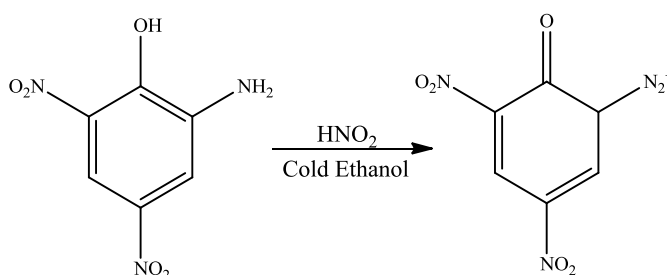
2.4 AZO COMPOUNDS

Azo compounds possess the functional group, $R-N=N-R'$, where R and R' can either be an alkyl or an aryl group. The International Union of Pure and Applied Chemistry (IUPAC) describes azo compounds as derivatives of diazene (diimide), $HN=NH$, which has both hydrogens substituted by alkyl or aryl groups (Gold *et al.*, 1997).

Aliphatic azo compounds are mostly colourless, whereas the aromatic counterparts possess variety of colours. The presence of the azo bond between the aromatic systems, helps extend the conjugation, leading to a chromophore being formed. Presence of groups such as $-OH$ and $-NH_2$ on the chromophore will result in the enhancing of the light absorbing property of the chromophore, shifting the wavelength of absorption higher into the visible region (400-800nm) of the electromagnetic spectrum. These groups are termed auxochromes (Solomons, 2012).

2.4.1 Origin

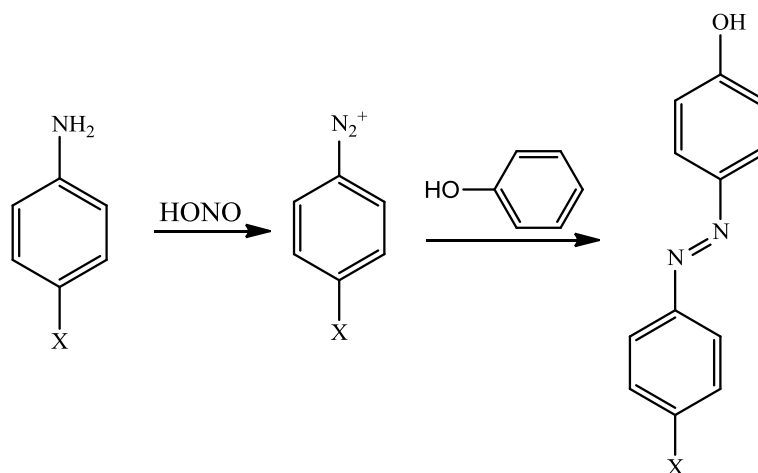
In 1858, Peter Griess reported on the synthesis of a new class of compounds. He was initially working on forming the hydroxy derivative of picramic acid. However, after slightly changing the conditions by employing cold alcoholic nitrous acid instead of warm nitrous acid (Scheme 2.2) he observed that the product had properties different from that of the expected product. A similar observation was made when other primary aromatic amines were used in place of picramic acid. He proposed that, the product was formed as a result of two atoms of nitrogen replacing two atoms of hydrogen. Hence, he called this new class of compounds, "*diazo*." Further work on the correct structure of the diazo compound formed revealed however that, $-\text{NH}_2$ was rather replaced by $-\text{N}_2$ (Gordon and Gregory, 2012, Regitz, 2012).



Scheme 2.2 Diazotization of Picramic acid by Griess

2.4.2 General Mechanism

Synthesis of *azo* compounds follows a two-step pathway: diazotization of the primary aryl amine in an acidic medium and coupling with an activated aryl species, such as naphthol, in a basic medium. The diazotization step takes place under acidic conditions at reduced temperatures, and the coupling agent is introduced under basic conditions. The general reaction for this reaction is illustrated in Scheme 2.3.



Scheme 2.3 General reaction pathway for the formation of azo dyes

2.5 BIOLOGICAL ACTIVITY OF AZO COMPOUNDS

The biological activity of *azo* compounds arises mostly from the particular metabolic pathways, the *in vivo* enzymatic reduction of the *azo* bonds. This leads to the cleavage of the *azo* bond resulting in the releasing of the aryl amine from which the *azo* dye originated. Depending on aryl amine, the resulting product may be more or less toxic than the parent *azo* dye (Chung *et al.*, 2008, Pandey *et al.*, 2007).

Azo dyes obtained from the benzidine (fig. 2.5), and its derivatives have been shown to possess higher toxicity. Research has demonstrated the carcinogenic activity of benzidine-based compounds (Makena and Chung, 2007, Chung *et al.*, 2000).

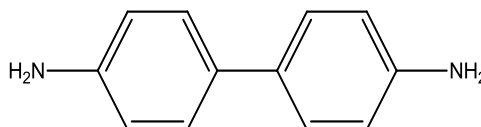


Figure 2.5 Structure of benzidine

The mutagenetic activity of benzidine and its analogues has been reported. For example, the action of intestinal microflorae in humans on the *trisazo* dye

Direct Black 38, fig. 2.6, releases the benzidine moiety (Sponza and Işık, 2005).

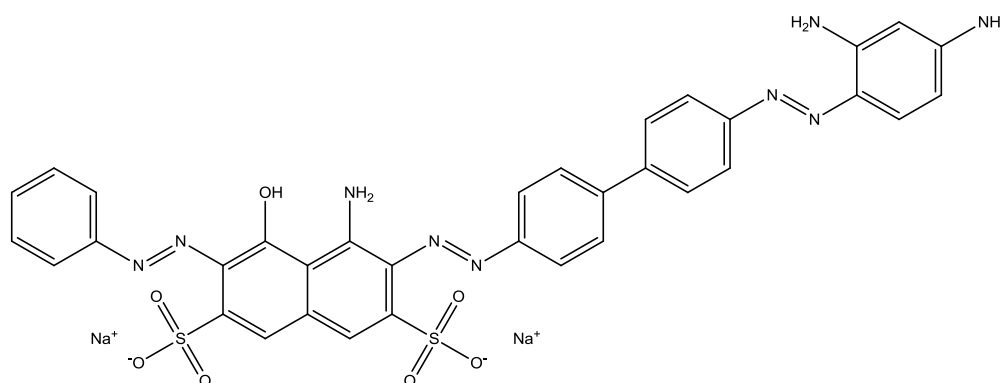


Figure 2.6 Structure of Direct Black 38

In spite of these potential toxicity of *azo* dyes, they also exhibit some encouraging biological activities, conferring on them significant medical use.

Azo dyes and their *in vivo* reduction products play a significant role in the treatment of colon disease such as colitis and irritable bowel syndrome, by acting as specific site delivery drugs. In these drugs, the reduction of the *azo* bond takes place in the colon, making them very site-specific. As a result, drug designers are able to develop target therapy medicines. As example is the *azo* derivative of 5-aminosalicylic acid immobilized on a polyethylene glycol (PEG) matrix, fig. 2.7, which possess anti-inflammatory and cytoprotective activity (Garjani *et al.*, 2004).

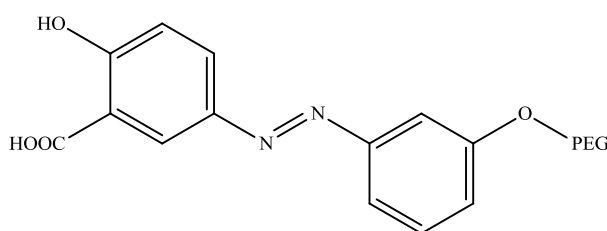


Figure 2.7 Structure of PEG immobilised on a dye

2.5.1 Antiviral Activity

The bisazo compound, known and referred to as FP-21399 (fig. 2.8) has demonstrated considerable anti-human immunodeficiency virus (HIV) activity. This drug works by blocking the entry of the virus into the CD4+ cells and also blocks the fusion of infested cells with the healthy ones. The CD4 (cluster differentiation 4) cell is a glycoprotein located on the outer surface of the white blood cells and helps fight infections. After ingestion, FP-21399 is found in much concentrations in the lymph nodes, where a high concentration of HIV and CD4+ are found.

This compound has been demonstrated to be active against all strains of the HIV virus as well as some few resistant strains. Clinical trials have confirmed the anti-HIV activity of the dye (Stellbrink, 2007, Ono *et al.*, 1997).

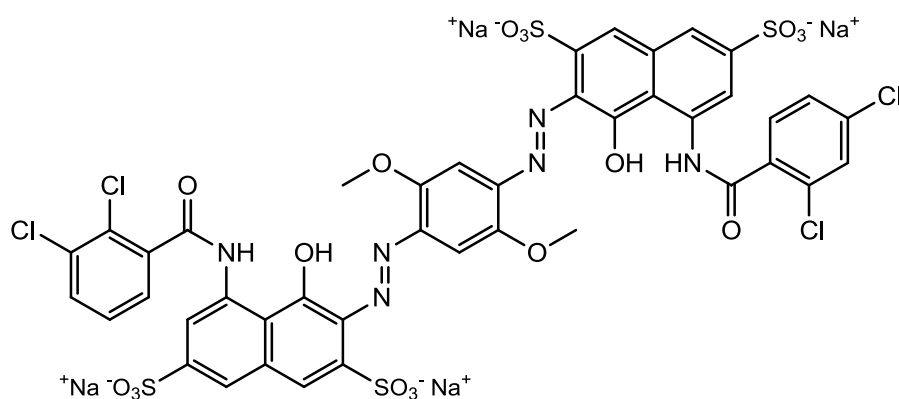


Figure 2.8 Structure of FP-21399

2.5.2 Anti-microbial activity of azo-containing Schiff bases

The versatility of azo compounds plays a vital role in both fundamental and research applications. Aside their chemical uses, azo-azomethine dyes are receiving considerable interest in the plastic, textile and leather sectors.

Azo compounds are able to coordinate with metal ions, the *azo* bond may or may not be involved in the coordination to the ion to form the chelate ring. The extensive use of Schiff base complexes results from the relative stability of such complexes. Metal chelates play vital role in the chemistry of living organisms, a large number of metal-proteins and other metal complexes in biological systems.

Salicylaldehyde-derived Schiff bases are polydentate ligands and form coordinates either in the neutral or the deprotonated ionic form. In a study, the antimicrobial potential of such bases was investigated. A number of Schiff ligands were synthesised and complexed with cobalt (II) and copper (IV) (fig. 2.9). The activity of both the ligands and the complexed compounds was determined. It was observed that the metal complexes generally exhibited greater activity against the test organisms than the base ligands. The partial sharing of the charge on the metal ion by the donor atoms leads to an increase in the lipophilicity of the compound, resulting in the increase in the ability of complex to permeate the lipid layer of the cell membrane of the organism. This accounts for the greater activity of the complexes over the ligands (Ispir, 2009).

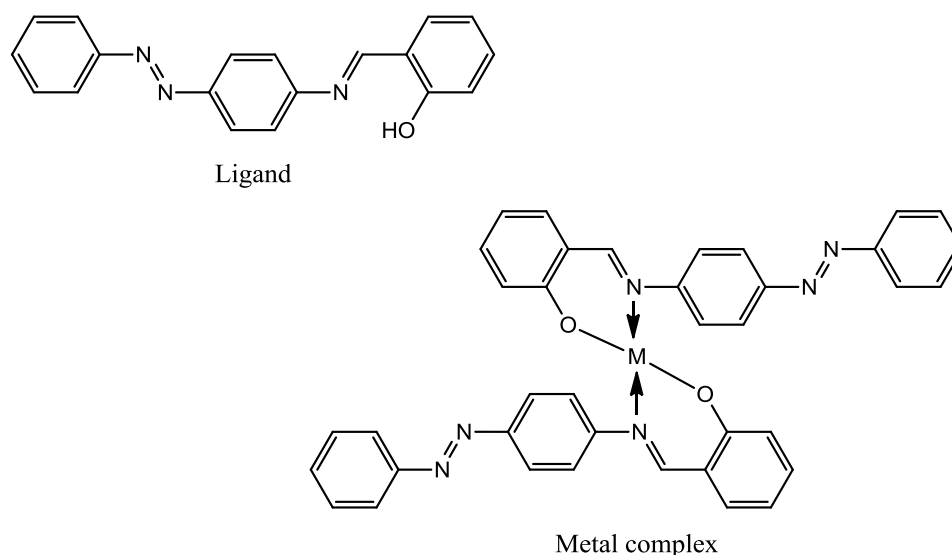


Figure 2.9 Structure of Schiff base ligand and metal complex

From the proposed structure of the complex, the *azo* bond is not involved in the coordination to the metal ion. As the *azo* bond cleaves to release the corresponding amines, the active portion of the dye (Section 2.1), two amines per each molecule of the complex as opposed to one by the ligand, will be released. This obviously explains the increased activity of the complexes – the complexation increasing the rate and ease of transport across cell wall of the organism and the sheer numbers of amines released causing the inhibition.

2.5.3 Anti-microbial activity of *azo*-containing heterocycles

Heterocycle *azo* dyes enjoy a vast range of use as dyestuff in the electronic industries. These applications include colorimetric sensors, nonlinear optical (NLO) devices and liquid crystal display (LCD) used as potential sensitizers for photodynamic therapy (PDT).

In recent times, focus has been shifted to incorporating of *azo* moiety into heterocycle systems. One of such system is 1,3,4-thiadiazole (fig. 2.10) and its derivatives. Antitumor, antibacterial, anti-inflammatory, antimycotic and

antifungal are some of the biological activities exhibited by this nitrogen containing heterocycle. This extensive broad spectrum activity have been attributed to the existence of the toxophoric –N-C-S moiety (Mavrova *et al.*, 2009).

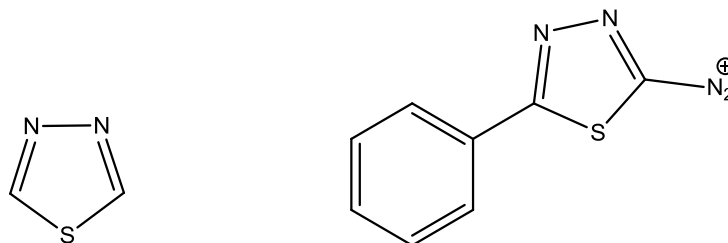


Figure 2.10 Structure of thiadiazole and diazonium salt derivative

Keerthi Kumar *et al* (2013) synthesised and screened for the antimicrobial activity of some *azo* dyes synthesised by the coupling of phenyl amino derivative of 1,3,4-thiadiazole (fig. 2.10) with both heterocyclic and non-heterocyclic aromatic systems. Since all the compounds contain the thiadiazole system, any observed activity may be attributed to the coupling agent. It was observed that the coupling agents with hetero atoms showed a higher activity against the various test organisms than their non-heterocyclic counterparts. For instance, the 8-hydroxyquinoline coupled dye (fig. 2.11) was much active against *S. aureus*, with an MIC of 25µg/ml, with the 2-naphthol dye having an MIC of 200µg/ml against the same organism. Also, an MIC of 50µg/ml and 400 µg/ml was obtained for the amino pyridine and methyl aniline dyes respectively against *P. aeruginosa*. This goes to show that the presence of the hetero atoms in the ring contributes to the observed activity of the dyes. (Keerthi Kumar *et al.*, 2013). The presence of the lone pairs of electrons on the hetero atom may have contributed to the observed activity of these compounds. However, there is the need to compare similar structured

heterocyclic compounds to investigate which will offer better activity, which will guide future drug development.

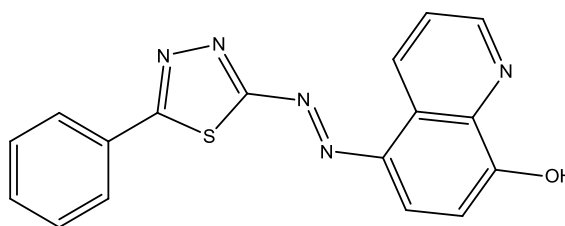


Figure 2.11 Structure of 8-hydroxy quinolone coupled thiazole derivative

Benzothiazole (fig. 2.12) and derivatives have demonstrated variety of biological activity, including antihistamine, antitumor and antibacterial.

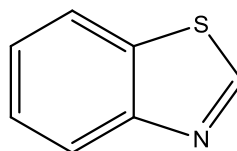


Figure 2.12 Structure of benzothiazole

Kumar *et al.* (2013) also investigated on the activity of various derivatives of phenyl amide and naphthols coupled with the amino benzothiazole. The methoxy derivative of the amide (fig. 2.13) showed a greater activity by inhibiting all test organisms. This can be attributed to the greater non-polar character of the ether functionality over the halogenated and nitro groups. Also the naphthol dyes exhibited a higher activity over the other phenolic counterparts. It can be said therefore that the extra aromatic ring on the naphthol enhances the lipid solubility of the dye (Keerthi Kumar *et al.*, 2013)

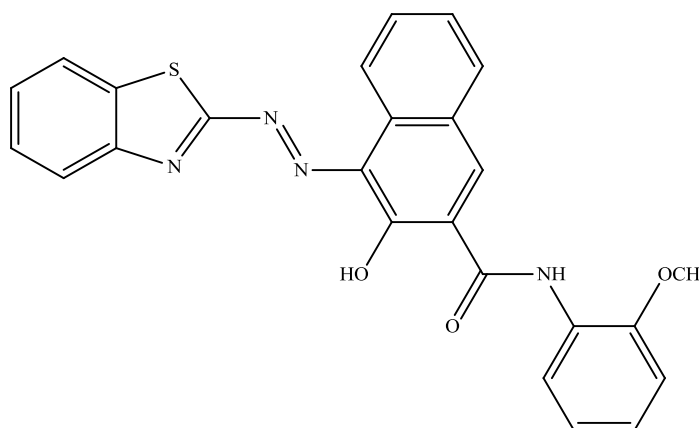


Figure 2.13 Structure of the benzothiazole coupled methoxy amide derivative

Although the methoxy derivative exhibited the greatest activity, careful investigation of the derivatives would reveal that the substitution pattern was not the same. For instance, the nitro derivative has the nitro substituent *para* to the amide bond. It is conceivable that steric hindrances will make the compound shown in fig 2.13 able to withstand modification by cell matter of some organism than if it were a *para* substituted. As a result for a more general and direct comparison to be made, the substituents should have been at the same positions.

2.5.4 Anti-microbial activity of naphthol azo dyes

Most dyes in use consist of the *azo* and naphthalene moieties. However their antimicrobial activity are less exploited.

Swati *et al.* (2011) studied the effect of substitution on various anilines coupled with 2-naphthol. It was observed that the carboxylic acid and hydroxyl aniline derivatives showed a greater antimicrobial activity. Also, the presence of a chloro group, *ortho* to the *azo* bond contributed nothing to the activity of the dye, the same MIC was obtained against all the test organisms

as the unsubstituted anilines. The methoxy derivative demonstrated a greater inhibition against the gram negative organisms used with *E. coli* being the most susceptible with an MIC of 35µg/ml obtained against this organism. The hydroxy derivative was more active against the gram negative *B. subtilis* with an MIC of 35µg/ml (Swati *et al.*, 2011).

In a recent study, the substituents effect of some naphthol and phenolic *azo* dyes were investigated. The 1-naphthol moiety was shown to be more active than the 2-naphthol and phenolic systems. As discussed earlier, the extra lipophilicity offered by the naphthol contribute to the higher activity over the phenol. The structures of the most active compounds, *p*-ABAαN and *p*-NAαN, are shown in fig. 1.2 (Sec 1.2)

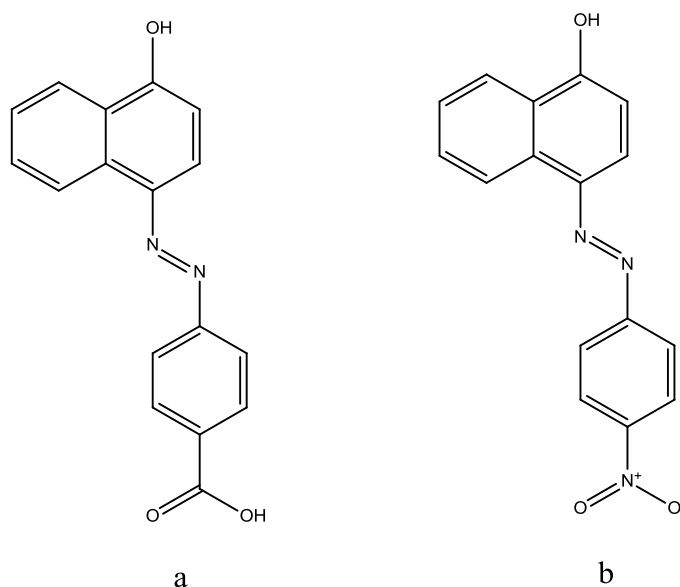


Figure 2.14 Structure of *p*-ABAαN (a) and *p*-NAαN (b)

Of the two, *p*-NAαN exhibited greater activity by recording a minimum inhibitory concentration (MIC) of 20µg/ml against *C. albicans* (Kofie *et al.*, 2015). The focus of the study was the investigation of the effect of substituents

on the activity. However, from the critical examination of the structures in fig 1.2, it can be observed that the carboxylic acid functional group, the hydroxyl group of the naphthol as well as the aromatic ring provides suitable sites for structural modification. Exploration of the possible modifications with the corresponding activity, therefore, forms the basis for this study.

CHAPTER THREE

MATERIALS AND METHODS

3.1 MATERIALS

3.1.1 Reagents

Table 3.1 Reagents and materials used with their sources

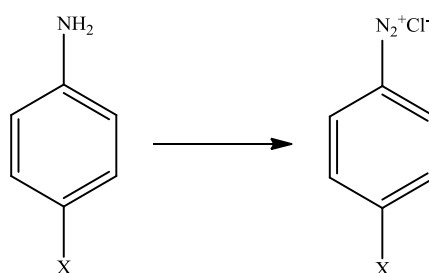
| Materials/Reagents | Source |
|--|-----------------|
| Petroleum ether 40/60 | BDH |
| 1-Naphthol | BDH |
| 2-chloro-4-nitroaniline | BDH |
| <i>p</i> -nitroaniline | BDH |
| 4-aminobenzoic acid | BDH |
| Ethyl- <i>p</i> -aminobenzoate | BDH |
| Ethyl acetate | BDH |
| Potassium hydroxide (KOH) | BDH |
| Ethyl bromide | BDH |
| Potassium iodide | BDH |
| Sodium nitrite | VWR Chemicals |
| Sodium thiosulphate penta hydrate | BDH |
| Sodium hydroxide | Fisher Chemical |
| Sodium chloride | BDH |
| Acetic anhydride | BDH |
| Hydrochloric acid | BDH |
| Hexane | Fisher Chemical |
| Silica gel pre-coated thin layer chromatography (TLC) plates | Alugram Sil G |
| Ethanol (96%) | BDH |
| Methanol | BDH |

3.1.2 Equipment and Instrument

The Infra-Red (IR) spectra were obtained with a PerkinElmer Spectrum Two Spectrometer in the 4000-400 cm^{-1} range. The ^1H NMR spectra were obtained with a Bruker 400 Spectrometer with a frequency of 400 MHz and the MS data were obtained with an Openlynx LCMS Generic Chromatograph. The melting points were determined by the open capillary method with a Stuart Digital SMP10 melting point apparatus. A reflux system with a circulator chiller and water bath from Buchi were also used. All structures were sketched with the aid of ChemDraw Ultra 12.0 software.

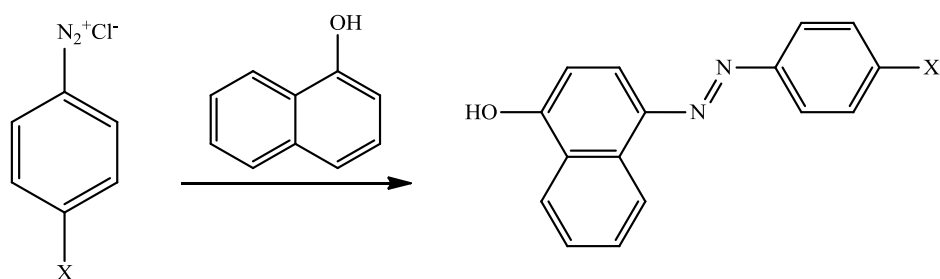
3.2 METHODS

3.2.1 General procedure for the formation of the diazonium salt



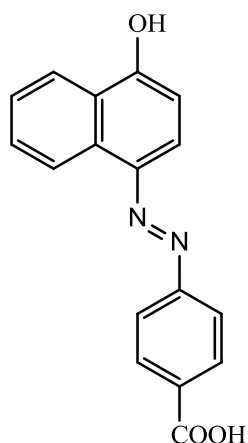
In a 250ml volumetric flask, primary aromatic amine (1 eq) was dissolved with a mixture of 15ml of 2M hydrochloric acid (HCl) and 5ml of water. The resulting solution was immersed in an ice bath and the temperature maintained below 5°C . 50ml of 1M sodium nitrite (NaNO_2) solution was added gradually to this solution with constant stirring whiles keeping the temperature below 5°C . Any precipitate formed was filtered off and discarded. The salt was covered and kept in the ice bath.

3.2.2 General procedure for the coupling reaction



In a 250ml beaker, 1 eq of 1-naphthol was dissolved in 50ml of 3M sodium hydroxide (NaOH), cooled to below 5°C by immersing in an ice bath with stirring. The cold diazonium solution was slowly added to the naphthol solution while stirring, ensuring that the temperature is always below 5°C . Coloured crystals of the azo compound developed. After the addition of all the diazonium salt, the mixture was left in the ice bath for about 30 minutes with occasional stirring. The mixture was suction filtered and the solid crude crystals dried. The crude was purified by either recrystallization from appropriate solvent or column chromatography and the pure compounds obtained and allowed to dry.

(E)-4-((4-hydroxynaphthalen-1-yl)diazenyl)benzoic acid



The product was obtained in (2.44g, 83.7%) as a dark brown solid.

Rf.: EtOAc: MeOH, 8:2 (0.64)

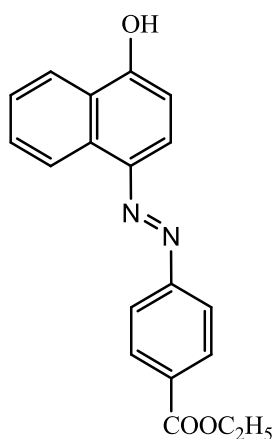
mp 287-289°C, Lit 288-290°C

IR (V_{\max} cm^{-1}): 3373.4, 1681.98, 1497.55, 1402.99, 1159.22, 1243.61.

^1H NMR (400MHz, DMSO-d_6) δ ppm: 6.90 (1H, d, $J=16\text{Hz}$, Ar- H_a), 8.1 (1H, d, $J=16\text{Hz}$, Ar- H_b) 8.78 (2H, d, $J=8.0\text{Hz}$, Ar- H_c), 8.23 (2H, d, $J=8.0\text{Hz}$, Ar- H_d), 8.17 (1H, d, $J=8\text{Hz}$, Ar- H_e), 7.86 (1H, d, $J=8\text{Hz}$ Ar- H_f) 7.97 (1H, m, Ar- H_g), 7.61 (1H, m, Ar- H_h).

m/z (ES): 293 ($\text{M}^+ + \text{H}$), 246.9 ($\text{M}^- - \text{CO}_2\text{H}$), 135.0 ($\text{M}^+ - \text{C}_{10}\text{H}_7\text{NO}$)

(E)-ethyl-4-((4-hydroxynaphthalen-1-yl)diazenyl)benzoate



The product was obtained in (2.395g, 74.8%) as a dark brown solid.

R_f : EtOAc: MeOH, 8:2 (0.57)

Mt pt. 245-247

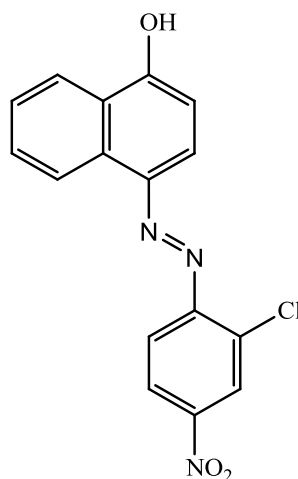
IR (V_{\max} cm^{-1}): 3376.82, 1380.25, 1169.33

^1H NMR: (400MHz, DMSO-d_6 , δ ppm): 1.23 (3H, t, $J=4.8$ Hz, CH_3), 4.1 (2H, q, $J=4.4$ Hz, CH_2), 6.15 (1H, d, $J=6.8\text{Hz}$, Ar- H_c), 7.60 (1H, d, $J=6.8\text{Hz}$, Ar- H_d), 8.72 (2H, d, $J=6\text{Hz}$, Ar- H_e), 7.90 (2H, d, $J=6\text{Hz}$, Ar- H_f), 8.15 (1H, d,

$J=3.6\text{Hz}$, Ar-H_g), 8.04 (1H, d, $J=4.0\text{Hz}$, Ar-H_h), 7.45 (1H, m, Ar-H_i), 7.19 (1H, m, Ar-H_j)

m/z (ES): 293 ($M^+ - \text{CH}_2\text{CH}_3$), 275.5 ($M^- - \text{C}_2\text{H}_5\text{O} + 1$), 247.0 ($M^- - \text{COOC}_2\text{H}_5 + 1$)

(E)-4-((2-chloro-4-nitrophenyl)diazenyl)naphthalen-1-ol



The product was obtained in (3.09g, 94.5%) as a dark reddish solid.

Rf.: EtOAc: MeOH, 8:2 (0.62)

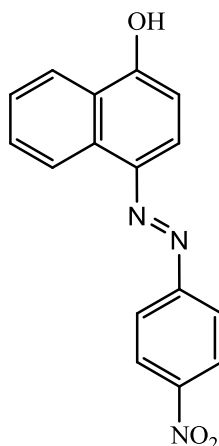
Mp: 183-185°C

IR (V_{max} cm^{-1}): 3378.14, 1637.35, 1584.75, 1538.05, 1512.76, 1406.79, 1276.23, 1168.6

^1H NMR: (400MHz, DMSO, δ ppm): 6.40 (1H, d, $J=4\text{Hz}$, Ar-H_a), 7.98 (1H, d, $J=4\text{Hz}$, Ar-H_b), 8.60 (1H, d, $J=4.4\text{Hz}$, Ar-H_c), 8.19 (1H, s, Ar-H_d), 8.41 (1H, d, $J=4.8\text{Hz}$, Ar-H_e), 7.40-7.30 (1H, m, Ar-H_f), 8.12-8.00 (1H, m, Ar-H_g), 7.65-7.50 (2H, m, Ar-H_h)

m/z (ES): 325.9 (M^-), 281.1 ($M^- - 46$), 183.9 ($M^- - 142$), 168.9 ($M^- - 157$)

(E)-4-((4-nitrophenyl)diazenyl)naphthalen-1-ol



The product was obtained as a dark brown solid in (2.61g, 88.9%)

Rf: EtOAc: MeOH, 8:2 (0.68)

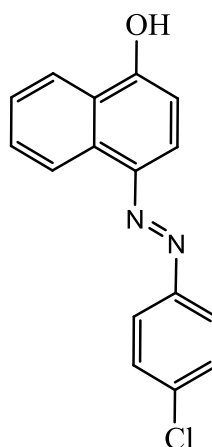
Mp. 124-126°C, lit 123-125°C

IR (V_{\max} cm^{-1}): 3367.1, 1594.29, 1502.28, 1258.74, 1167.5.

^1H NMR: (400MHz, DMSO, δ ppm): 6.82 (1H, d, $J=8\text{Hz}$ Ar- H_a), 8.09 (1H, d, $J=8\text{Hz}$, Ar- H_b), 8.53 (2H, d, $J=7.2\text{Hz}$, Ar- H_c), 8.33 (2H, d, $J=7.2\text{Hz}$, Ar- H_d), 8.46 (1H, d, $J=5.6\text{Hz}$, Ar- H_e), 7.83 (1H, m, Ar- H_f), 7.66 (1H, m, Ar- H_g), 7.76 (1H, d, $J=5.6\text{Hz}$, Ar- H_h).

m/z (ES): 292.0 (M^- , 100%) 137.0 ($\text{M}^- - \text{C}_6\text{H}_4\text{N}_2\text{O}_2+1$), 144.8 ($\text{M}^- - \text{C}_{10}\text{H}_8\text{O}$)

(E)-4-((4-chlorophenyl)diazenyl)naphthalen-1-ol



The product was obtained in (2.69, 95.4%) as a dark brown solid.

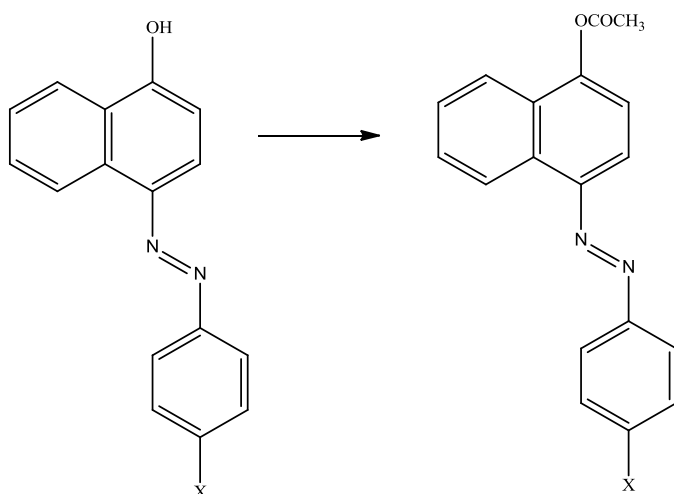
Rf.: EtOAc: MeOH, 8:2 (0.65)

IR (V_{\max} cm^{-1}): 3300, 1596.69, 1479.22, 1404.11, 1272.28, 1155.61.

^1H NMR: (400MHz, DMSO, δ ppm): 6.98 (1H, d, $J=12\text{Hz}$ Ar-**H_a**), 7.85 (1H, d, $J=12\text{Hz}$, Ar-**H_b**), 7.66 (2H, d, $J=10\text{Hz}$, Ar-**H_c**), 8.64 (2H, d, $J=10\text{Hz}$, Ar-**H_d**), 7.52-7.48 (2H, m, Ar-**H_e**), 8.02-7.97 (2H, m, Ar-**H_f**)

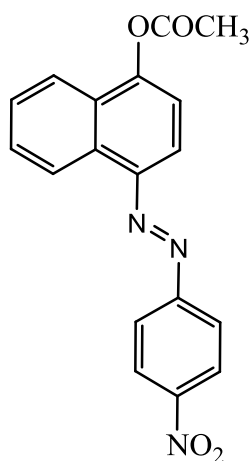
m/z (ES): 282.9 (M^+ , 100%), 298.8 ($\text{M}^+ + \text{H}_2\text{O}$), 138.9 ($\text{M}^- - \text{C}_{10}\text{H}_7\text{O}$)

3.2.3 Procedure for formation of the acetylated products



In a 150ml round bottom flask, 5ml of 25% NaOH was added to the *azo* compound (1 eq) and stirred for 15 minutes at room temperature. To the resulting solution, acetic anhydride (1 eq) was added and stirred for a further 1 hour at room temperature. The solid crude was filtered off and washed with cold water. The pure crystals was obtained after recrystallization from ethanol and ethyl acetate.

(E)-4-((4-nitrophenyl)diazenyl)naphthalene-1-yl acetate



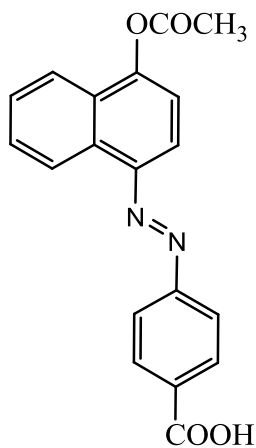
The product was obtained as a dark brown solid in (250mg, 74.6%)

Rf.: Pet: EtOAc, 6:4 (0.61)

Mp. 147-150°C

IR (V_{\max} cm^{-1}): 3267.51, 1628.23, 1594.61, 1547.6, 1502.56, 1259.51.

(E)-4-((4-acetoxynaphthalen-1-yl)diazenyl)benzoic acid



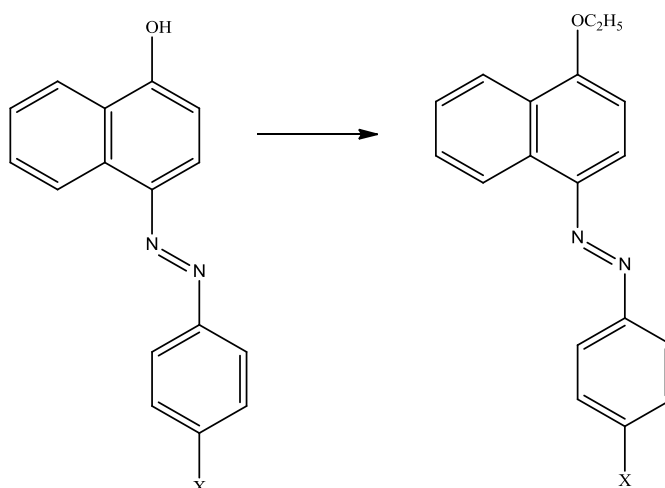
The product was obtained as a dark brown solid in (238mg, 71.3%).

Rf.: Pet: EtOAc, 6:4 (0.54)

Mp. 250-252°C

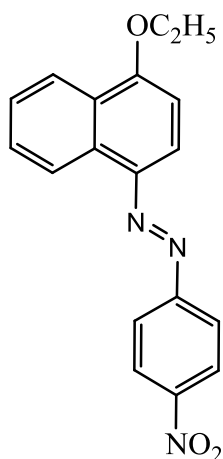
IR (V_{\max} cm^{-1}): 3359.22, 1738.21, 1497.55, 1402.99, 1159.22, 1243.61

3.2.4 Procedure for the formation of the alkylated products



In a 150 ml round bottom flask, 10 ml of methanol was added to the *azo* dye (1 eq). 5 ml of 25% KOH was added and stirred at room temperature for 15 minutes. To this solution, ethyl bromide (2 eq) and potassium iodide (1.5 eq of ethyl bromide) was added and stirred for two hours at 90-95°C. The mixture was then transferred into a separatory funnel and shaken with 25 ml of 1M sodium thiosulphate solution. The organic layer was then extracted with three 15 ml portions of ethyl acetate, washed with saturated sodium chloride solution and dried. The crude was purified by recrystallization from ethanol (70%).

(E)-1-(4-ethoxynaphthalen-1-yl)-2-(4-nitrophenyl)diazene



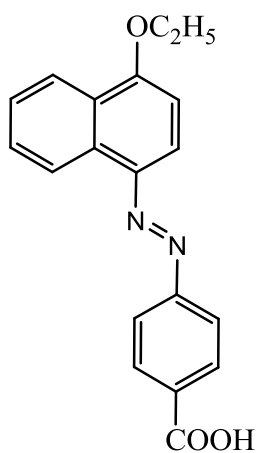
Using the above procedure, the product was obtained in (252mg, 78.5%) as a dark solid.

Rf.: Hexane: EtOAc, 9:1 (0.71)

Mp. 121-123°C

IR (V_{\max} cm^{-1}): 1486.9, 1254.26, 1210.15, 1147.19.

(E)-4-((4-ethoxynaphthalen-1-yl)diazenyl) benzoic acid



The product was obtained as dark brown solid in (252mg, 72.7%)

Rf.: Hexane: EtOAc, 9:1 (0.65)

Mp. 102-104°C

IR (V_{\max} cm^{-1}): 3359.22, 1738.21, 1497.55, 1402.99, 1159.22, 1263.25

3.2.5 Antimicrobial Assay

Various concentrations of the synthesised compounds (5000, 2500, 1250, 625, 312.5, 156.25, 78.13, 39.07 $\mu\text{g}/\text{mL}$) were prepared by serial dilution using methanol: water (50:50) as diluting solvent.

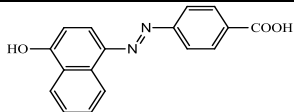
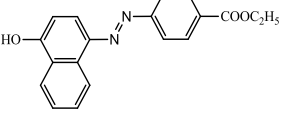
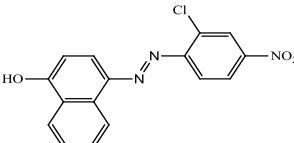
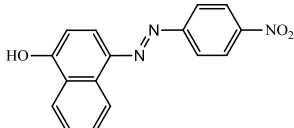
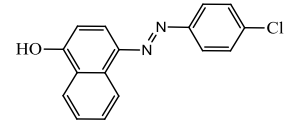
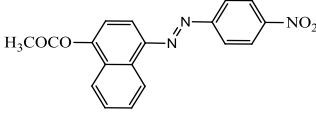
Using a micropipette, 100 μL of the sterile nutrient broth was transferred into each well of the micro titre plate. 90 μL of each of the test solution was added to the broth in the wells and labelled appropriately. 10 μL of each of the test microorganism was then dispensed into the appropriate well and the plate covered and incubated at 37°C for 18-24 hours. After the inoculation, the resultant concentration of the test compounds in each well were 2250, 1125, 562.50, 281.25, 140.63, 70.32, 35.16 and 17.58 $\mu\text{g}/\text{mL}$. The results were recorded and the Minimum Inhibitory Concentration (MIC) determined for each test compound.

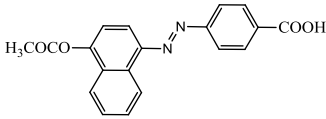
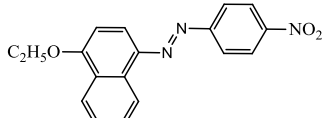
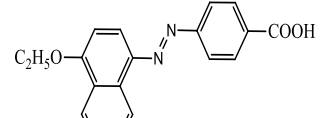
CHAPTER FOUR

RESULTS

4.1 SYNTHESIS

Table 4.1 Synthesised azo compounds with their physical data

| Compound | Code | Mol. Weight | % Yield | Melting pt, °C | R _f |
|---|--------|-------------|---------|---------------------------------|----------------------|
|  | KA 001 | 292.29 | 83.7 | 287-289°C (EtOAc:EtOH) | 0.64 (EtOAc:MeOH) |
|  | KA 002 | 320.34 | 74.8 | 245-247 | 0.57 (EtOAc:MeOH) |
|  | KA 003 | 327.74 | 94.5 | 183-185 (CH ₃ Cl) | 0.62 (EtOAc:MeOH) |
|  | KA 004 | 293.28 | 88.9 | 124-126 (EtOAc) | 0.68 (EtOAc:MeOH) |
|  | KA 005 | 282.72 | 95.4 | 151-154 (EtOH) | 0.65 (EtOAc:MeOH) |
|  | KA 006 | 335.31 | 74.6 | 147-150 (EtOAc:EtOH) | 0.61 (Pet:EtOAc) |

| | | | | | |
|---|--------|--------|------|---------------------------|------------------------|
|  | KA 007 | 334.33 | 71.3 | 250-252 (EtOAc:EtOH) | 0.54 (Pet:EtOAc) |
|  | KA 008 | 321.33 | 78.5 | 121-123 (Hexane:EtOAc) | 0.71 (Hexane:EtOAc) |
|  | KA 009 | 320.34 | 72.7 | 102-104 (Hexane:EtOAc) | 0.65 (Hexane:EtOAc) |

From Table 4.1, all the synthesised dyes were purified by recrystallization from their respective solvents, except KA 002 which was column chromatographed on silica gel. The solvents underneath the melting point values represent the solvents from which recrystallization was done.

4.2 ANTIMICROBIAL ASSAY

Table 4.2 Minimum Inhibition Concentrations (MIC) of the synthesised dyes

| Organisms | MIC ($\mu\text{g/ml}$) | | | | |
|--------------------------|--|---------------------|-----------------|----------------------|--------------------|
| | <i>S. aureus</i> | <i>S. pyrogenes</i> | <i>S. typhi</i> | <i>P. aeruginosa</i> | <i>C. albicans</i> |
| KA 001 | 562.5 | 562.5 | 1125 | 281.5 | 140.13 |
| KA 002 | 70.32 | 281.5 | 281.5 | 562.5 | 281.5 |
| KA 003 | 140.63 | 140.63 | 70.32 | 140.63 | 70.32 |
| KA 004 | 281.5 | 140.63 | 140.63 | 281.25 | 70.32 |
| KA 005 | 1125 | 562.5 | 562.5 | 140.63 | 281.50 |
| KA 006 | 1125 | 281.5 | 281.5 | 140.63 | 281.50 |
| KA 007 | 281.5 | 140.63 | 1125 | 562.50 | 562.50 |
| KA 008 | 70.32 | 35.16 | 70.32 | 35.16 | 70.32 |
| KA 009 | 140.63 | 140.63 | 70.32 | 70.32 | 140.63 |
| Cefuroxime axetil | 70.32 | 35.16 | 35.16 | 35.16 | 70.32 |

All the synthesised compounds demonstrated encouraging antimicrobial activity, with the alkylated derivatives being the most active compounds. Acetylation results in the formation of a less active compound. Replacing the nitro group in KA 004 with a chloro group leads to a reduction in the activity.

CHAPTER FIVE

DISCUSSIONS, CONCLUSION AND RECOMMENDATIONS

5.1 DISCUSSION

5.1.1 Synthesis

Azo compounds have been shown to possess a variety of biological activity including antimicrobial, antiviral, and antifungal among others. The first report of the synthesis of an *azo* compound happened in 1856. However, the derivatization of these compounds is largely unexplored. Recently in our research group, a number of *azo* compounds were synthesised and two of these dyes exhibited encouraging antimicrobial activity, fig. 5.1 (Sec 1.2).

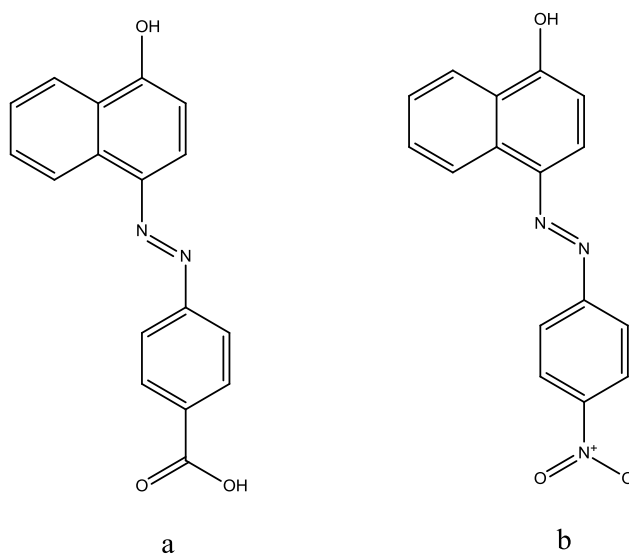


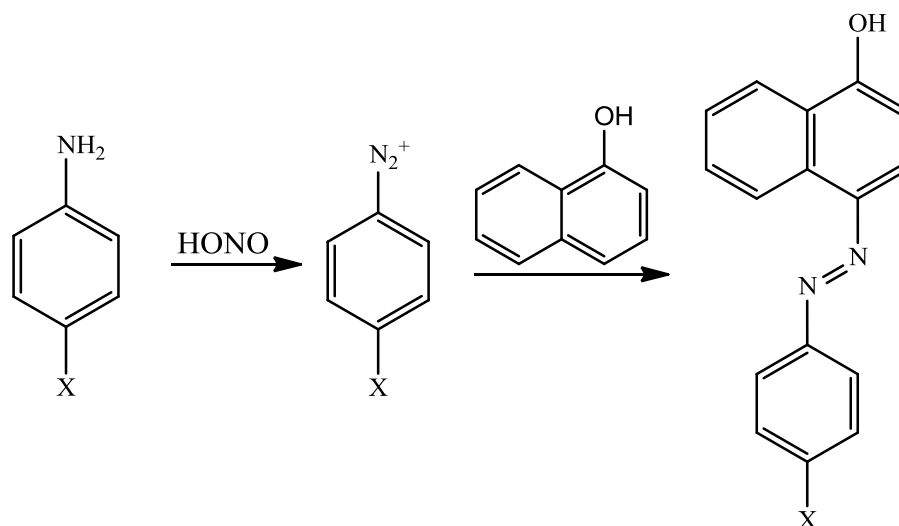
Figure 5.1 Structure of *p*-ABAaN (a) and *p*-NAaN (b)

As a medicinal chemist, considering the structure of the two compounds, the hydroxyl group on the naphthol provide a suitable site for structural modifications, such as the formation of an acetylated and alkylated derivatives of the dyes. Also, the presence of the carboxylic acid in *p*-ABAaN makes it favourable for the esterification of this compound. The substitution with a

halogen on the aromatic ring of *p*-NAαN is also a possible structural transformation to be explored.

The Directly Coupled Dyes

By employing the direct and well known route, the coupling between the diazonium salt and naphthol under carefully controlled conditions of temperature and pH, five *azo* compounds were successfully synthesised and in very good yield. The general scheme for this process is shown in scheme 5.1 (section 2.4.2)



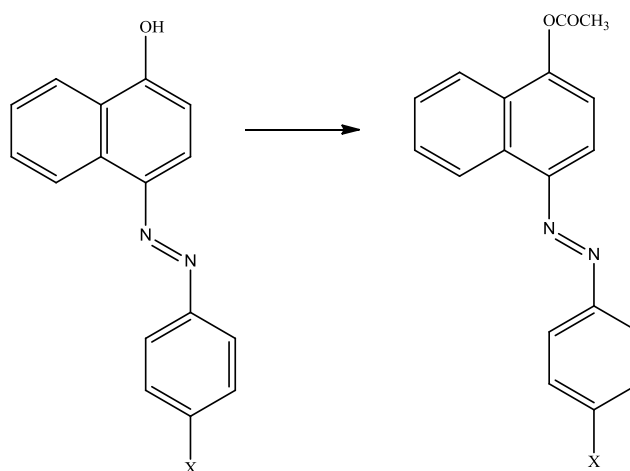
Scheme 5.1 General reaction pathway for the formation of azo dyes

The formation of the diazonium salt was detected by the instantaneous formation of a blue-black colour when a drop of the solution was tested with a potassium starch-iodide paper. The blue colour formed gave an indication of the presence of excess nitrous acid.

The Acetylated Products

The acetylation products were obtained by the general scheme (Sec. 3.2.3). This method for the acetylation was used in this work, owing to the readily availability of the reagents as well as the time taken to run the whole

experiment. From literature, a non-solvent method with a very high yield requires the use of a specialised catalyst, polystyrene-supported dimethylaminopyridine (DMAP). Also this procedure requires a maximum of 69 hours to produce the product. Coupled with the unavailability of the catalyst, the procedure used in this work requires stirring at room temperature to obtain the desired products.



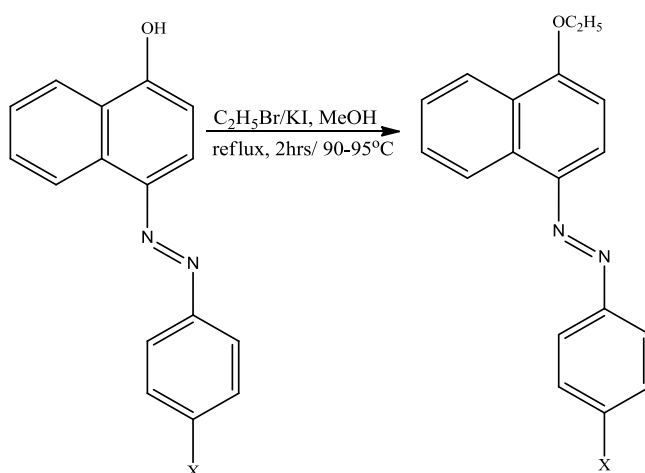
Scheme 5.2 General scheme for the synthesis of the acetylated products

The Alkylated Products

The alkylated products were synthesised *via* the Williamson's synthesis procedure, the synthesis of an ether from an alcohol and alkyl halide, scheme 4.2. From our preliminary work, it was observed that when sodium hydroxide (NaOH) was used in the deprotonation of the hydroxyl of the naphthol, after reaction with the alkyl halide, a product with a lower *r_f* than the starting material resulted. The implication of this was that the product formed was more polar than the starting material, which should not be the case since the ether product is expected to be less polar than the alcoholic starting material. To explain this observation, it can be said that the ether product formed was again hydrolysed by any excess NaOH, which is a much stronger base, present

in the reaction mixture, leading to the formation of the deprotonated naphthol product, which is more polar than the starting naphthol material, as shown in appendix J. As a result, a milder base, potassium hydroxide (KOH) was used.

Also, potassium iodide was added to the reaction mixture to convert the ethyl bromide to a more reactive ethyl iodide *in situ*. This conversion is referred to as the Finkelstein reaction (Caron, 2011). This conversion leads to the formation of molecular iodine which is non-polar. In order to easily separate the formed iodine from the desired product, sodium thiosulphate was added to convert the non-polar iodine into a more polar iodide form and extracted into the aqueous phase.



Scheme 5.3 General scheme for the synthesis of the alkylated products

5.1.2 Spectral Analysis

Directly Coupled Compounds

The Infra-Red (IR) region of the electromagnetic spectrum covers the range 4000 – 400 cm^{-1} . Interaction between the molecules and light of this wavelength provides important information about the functional groups present in the molecule.

From the IR spectrum for compound KA 001 (appendix A1), some major functional groups can be identified by their absorption bands. For instance, the free hydroxyl group the carboxylic acid functionality (-COOH) is indicated by the presence of a broad band peaking at 3373.4 cm^{-1} which slopes into the –CH stretching vibrational region at $\sim 3000 \text{ cm}^{-1}$. The absorption at 1681.98 cm^{-1} indicates the presence of a carbonyl (-C=O) of the carboxylic acid. The vibrational frequency for the *azo* bond (-N=N-) can be observed at 1497.55 cm^{-1} . Vibrational frequencies at 1243.61 cm^{-1} and 1159.22 cm^{-1} represent the –C-O vibrations for the carboxylic acid and naphthol respectively. The C-O of the acid will vibrate at a slightly higher frequency as the alternating of the proton on the two oxygen atoms introduces a slight double bond character into this bond. At this point, it is important to state that this results are consistent with that obtained by Kofie *et al.* (2015).

Mass Spectrometry (MS) differs from the other spectroscopic methods, in that whiles the other methods (IR, UV-Vis and NMR) studies the interaction between the molecules with electromagnetic radiations, in MS, interaction between the molecules with high energy electrons is of interest. This provides useful data about the molecular weight of the molecule. Electrospray

ionization is used in this work because fragmentation is reduced hence the possibility of obtaining the molecular ion peak.

From the MS data for the synthesised compounds, it is important to state that generally, they can be ionised in both the positive and negative modes, producing similar peak intensities in both modes. This is not far-fetched, given that the hydroxyl group on the naphthol can be protonated and deprotonated easily.

Examining the spectrum for KA 001, appendix A2, intense signals are obtained in the positive ionization mode (MS ES⁺ : 293, 1.4×10^6) and negative mode (MS ES⁻ : 291×10^6). In the negative mode, an intense peak is observed at m/z of 291.0 which represents an [M-H]⁻ peak. The molecular weight for this compound is predicted as 292, hence the loss of a proton will result in the formation of a fragment, approximately having a molecular weight of 291. A peak at m/z ratio of 292.9 in the positive mode further, representing the [M+H]⁺ ion confirms the molecular weight of the compound. The molecular ion peaks in both modes are shown in fig 5.2.

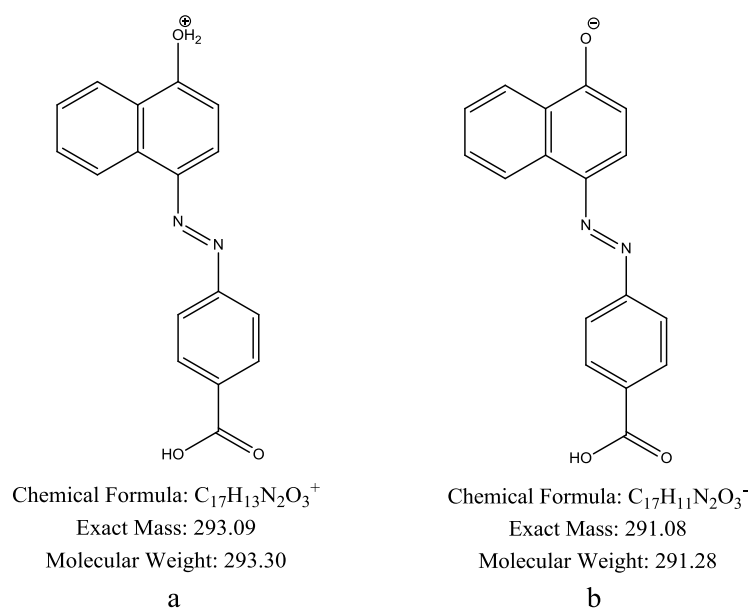


Figure 5.2 Molecular ion in a) positive and b) negative ionization modes

Again, a very intense peak is observed in the positive mode at m/z of 126.0 corresponding to the fragmentation of the naphthalene moiety (fig 5.2). A peak is observed at m/z of 128, which can be attributed to the $[X+2]^+$ peak. This is not far-fetched, since the uptake of 2 protons will result in the formation of the neutral naphthalene molecule. This fragment as a matter of fact is present in the spectra of all the other compounds as well. In addition, a peak corresponding to the loss of the carboxylic acid unit (-COOH) is observed at m/z of 246.9. The obtained fragment is shown in fig 5.3.

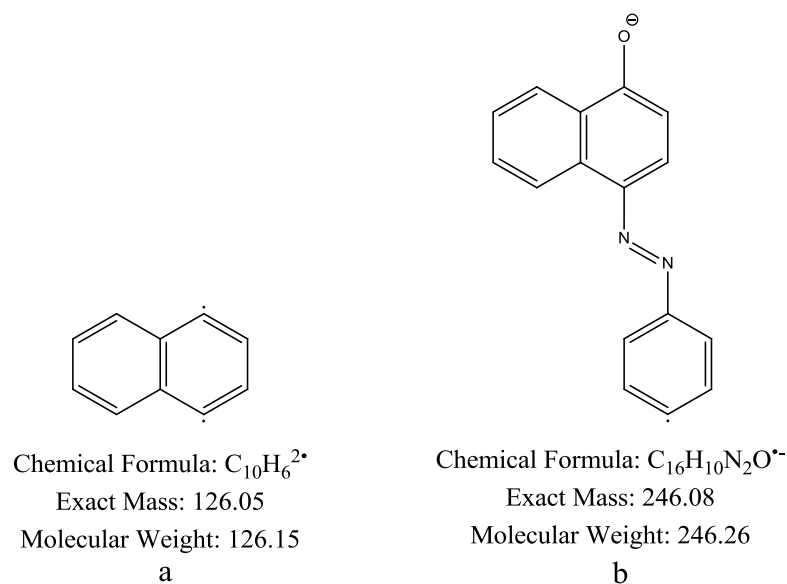


Figure 5.3 Fragment (ion) with m/z of 126.0 (a) and 246 (b)

For a chemist to understand the properties of a compound, it starts by being able to know the structure of the said compound. In recent years, X-ray crystallography has emerged as the tool of choice for determining the complete molecular structure of pure crystalline compounds. NMR spectroscopy follows by aiding the chemist with a direct and general tool for the elucidating the structures of both pure compounds and mixtures, either in solid or liquid forms. In NMR, the magnetic property of the nuclei of the atoms in the compound is harnessed to give information about the chemical shift and splitting patterns to provide useful information about the structure of the compound.

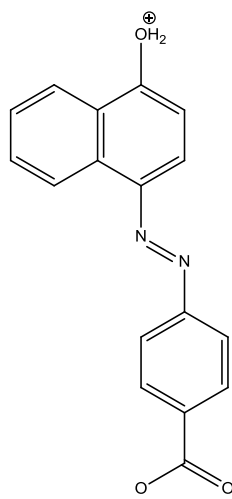
From the 1H NMR spectrum for the compound, appendix A3, a signal at a chemical shift of about 12 was expected for the carboxylic acid proton (-COOH). However, this signal is absent, which can be attributed to the fact that looking at the spectrum, it cover from 0 – 9.5 ppm. Also, the naphthol -OH, can be seen to have been superimposed by the signal due to water. That

notwithstanding, two doublet signals at chemical shift 6.9 and 8.1 both having integration for 1H are assigned to the protons at C-3 and C-4 respectively. This assignment results from the fact that C-4 proton is closer to the much more electronegative –OH group hence will experience a greater deshielding effect hence it appearing further downfield than the C-3 proton. Two doublet signals with integration for 2H at 8.78 and 8.23 are attributed to the protons at C-1 and C-2 respectively. In this case too, the proximity of the C-1 proton to the deshielding –COOH group shift it further downfield in the spectrum. Again, two doublets are 8.17 and 7.86 both with integration for 1H are assigned protons at C-5 and C-8 respectively. Here also the C-5 proton can be seen to be closer to a deshielding hydroxyl group, hence the assignment. Finally, there are two multiplet signals resulting from the C-6 and C-7 protons at 7.87-7.85 and 7.67-7.64 respectively.

For the compound KA 002, from the IR spectrum (appendix B1), a broad band at 3376.82 cm^{-1} signifies the absorption vibrations of the naphthol –OH. There is a –C=O absorption at about 1720 cm^{-1} which gives an indication of the presence of an ester functional group. When compared with that of KA 001, the carbonyl for the ester vibrates at a higher wavenumber than that of the carboxylic acid. This results from the fact that in the carboxylic acid, the hydrogen atom alternates between the two oxygen atoms. This leads to the introduction of a somewhat single bond character in its carbonyl functionality, reducing the energy required to cause vibrations in this molecule.

To compliment this observation, the MS for the compound was obtained, appendix B2. The molecular weight for this compound is predicted to be 320.

A molecular ion peak occurring at m/z of 321 in the positive mode and 319 in the negative mode was expected. However this is not observed, and can be attributed to the fact that ester linkages are generally weak bonds and breaks relatively easily. This fact can be ascertained by the presence of an intense peak at m/z ratio of 293.0 resulting from the cleavage of the ethyl ($-C_2H_5$) group, an $[M-X]^+$ ion, resulting in the formation of the carboxylate ion (fig 5.4). A similar fragment with an m/z of 291.0 corresponding to the $[X-H]^-$ in the negative mode.



Chemical Formula: $C_{17}H_{12}N_2O_3^{*+}$

Exact Mass: 292.08

Molecular Weight: 292.29

Figure 5.4 Fragment (ion) with m/z of 292.3

There is a peak at m/z of 247.0 which can be attributed to the $[M-COOC_2H_5+1]^-$ fragment. A peak at m/z of 177.2 can be attributed to the fragment obtained after the cleavage of the naphthol system. These two fragments are shown in fig. 5.5.

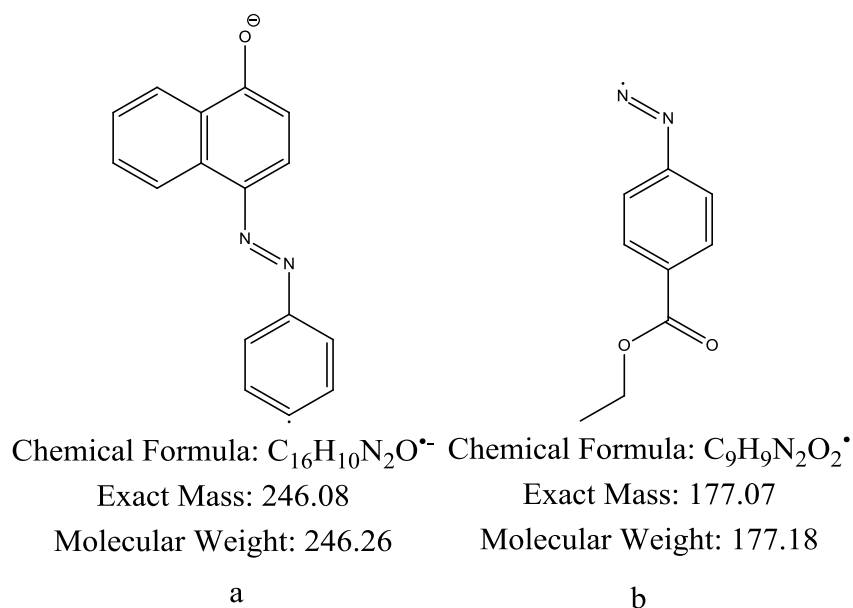


Figure 5.5 Fragment (ion) with m/z of (a) 246.3 and (b) 177.2

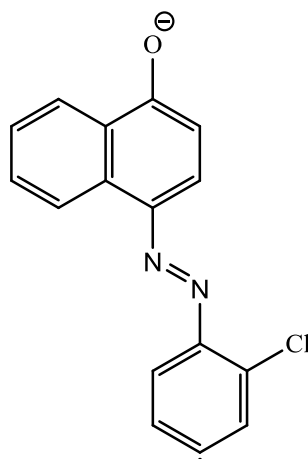
Investigation of the ¹H NMR spectrum for this compound, appendix B3, revealed the presence of a triplet signal, with an integration for 3H, at the chemical shift of 1.23 resulting from the protons on the methyl group (C-1). A quartet signal due to the methylene (-CH₂-) protons, is also observed at chemical shift 4.1 with an integration for 2H. The quartet signal arising from the splitting experienced by the neighbouring protons on the methyl group on C-1. Also a chemical shift of 6.15 and 7.60 corresponds to the signals of the protons at C-3 and C-4 respectively, both integrated for 1H. The strongly deshielding effect, results in the downfield shift of the C-4 signal, as a result of the close proximity to the hydroxyl group. Two doublets, with integration for 2H each, corresponding to the C-5 and C-6 protons appear at 7.90 and 8.72 respectively. Again, here too, the ester functional group causes the downfield shift of the C-6 protons. In addition, two doublets corresponding to the C-7 and C-8 protons are observed at 8.15 and 8.04. The signal due to the proton at C-7 appears downfield due to its closeness to the strong deshielding hydroxyl

group. As expected, there are multiplet signals at shifts 7.45 and 7.19 for the C-9 and C-10 protons respectively. The multiplet signal is not far-fetched since each proton is coupled to two other protons.

The IR spectrum for compound KA 003 can be located at appendix C1. From this spectrum, a broad band at 3378.14 indicates the presence of the naphthol –OH group. A peak at 1584.57 cm^{-1} indicates the presence of the nitro (-NO₂) functional group, with the –C-N vibrations appearing at the 1242.36 cm^{-1} . Strong bands at 894.74 and 832.43 cm^{-1} , representing –C-Cl vibrations, give indication of the presence of the chloro group in the compound.

Analysis of the MS data of the compound (KA 003), appendix C2, provided the following observations on the structure for the compound. There is a peak at m/z of 327.9 represented the molecular ion peak, [M+H]⁺, since the molecular weight for the compound is predicted to be 327, hence a gain of a proton in the positive mode will lead to the formation of the molecular ion. There is another peak at m/z of 329.9 with a percentage abundance of almost a third that at 327.9. This gives an indication of the presence of an isotopic atom, the chlorine atom. The chlorine atom exist naturally as the isotopes ³⁵Cl and ³⁷Cl in the abundance ratio of 75:25 (³⁵Cl: ³⁷Cl). This observation is repeated in the negative mode as well.

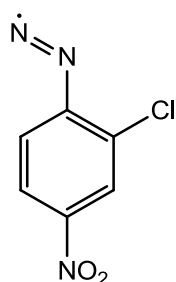
The cleavage of the nitro group results in the formation of a fragment (fig 5.6) with m/z of 280.0. Another at m/z 281.1 can be attributed to the formation of an [X+1]⁻ for this particular fragment.



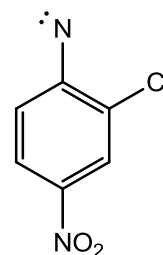
Chemical Formula: C₁₆H₉ClN₂O[⊖]
 Exact Mass: 280.04

Figure 5.6 Fragment with m/z of 280.0

In addition, at m/z of 168.9, a peak that can be associated with an [X-H][⊖] fragment resulting from the cleavage of the *azo* bond. The loss of the naphthol moiety will result in the fragment with an m/z of 183.9. These fragments are shown in fig 5.7.



Chemical Formula: C₆H₃ClN₃O₂[⊖]
 Exact Mass: 183.99



Chemical Formula: C₆H₃ClN₂O₂^{2⊖}
 Exact Mass: 169.99

Figure 5.7 Fragment (ion) with m/z of (a) 183.9 and (b) 169.9

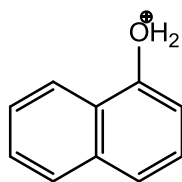
To confirm all this observations, the ¹H NMR spectrum was obtained, appendix C3. From the spectrum, a singlet is observed at the chemical shift of 8.19, with integration for 1H, which is as a result of the proton at C-2. The

other two protons at C-5 and C-6 are observed as doublets at chemical shifts 8.60 and 8.41 respectively. The C-6 experiences strong deshielding by the nitro group, hence the downfield shift. The spectrum can be seen at appendix C3.

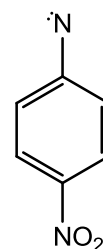
From the IR spectrum for KA 004, located at appendix D1, vibrational peaks obtained at 1547.51 cm^{-1} signifies the presence of the $-\text{NO}_2$ functional group accompanied by the $-\text{C-N}$ vibration at 1258.74 cm^{-1} .

The MS data for this compound can be located at appendix D2. The molecular weight for this compound is calculated as 293. In the positive mode therefore, the peak at m/z of 293.9 can be attributed to the $[\text{M}+\text{H}]^+$. In the negative mode, an $[\text{M}-\text{H}]^-$ fragment is indicated at the m/z of 292.0 with an $[\text{M}-\text{H}+1]^-$ peak at 293.0.

An $[\text{X}+1]^+$ fragment, corresponding to the ion due to the naphthol moiety is observed at m/z of 144.8 in the positive mode. Also, the cleavage at the *azo* bond will result in a fragment with m/z of 137.0. These two fragments are shown in fig 5.8.



Chemical Formula: $\text{C}_{10}\text{H}_8\text{O}^+$
Exact Mass: 144.06
Molecular Weight: 144.17



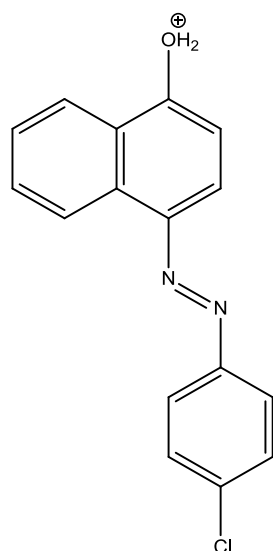
Chemical Formula: $\text{C}_6\text{H}_4\text{N}_2\text{O}_2^{2\bullet}$
Exact Mass: 136.03
Molecular Weight: 136.11

Figure 5.8 Fragment (ion) with m/z of 144.8 (a) and 137.0 (b)

From the ^1H NMR spectrum, appendix D3, it can be observed that the singlet that was obtained in the spectrum for KA 003 is absent in this particular case. This further confirms the absence of the chloro group. Also, there are two doublets each with an integration for 2H at chemical shifts 8.53 and 8.33 for the protons C-2 and C-3 respectively. Again, here, the $-\text{NO}_2$ causes the downfield shifting of the C-2 protons.

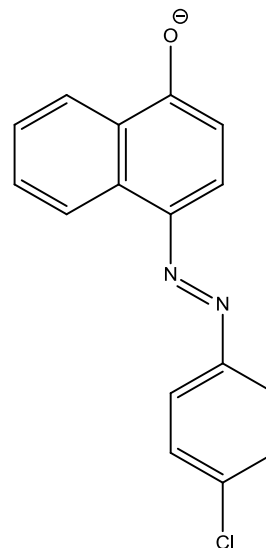
From the IR spectrum for compound KA 005, appendix E1, a peak at 824.05 cm^{-1} in the fingerprint region, is as a result of the vibrations of a C-Cl bond. This indicates the presence of the chloro group in this compound.

To compliment this observation, the MS data was obtained, appendix E2. The calculated molecular weight for the compound is 282, hence peaks at m/z of 281.0 and 282.9 in the negative and positive modes respectively can be said to the molecular ion peaks each mode. The isotopic chlorine group is shown by the appearance of peaks with about a third the abundance of the molecular ion at 283.0 and 284.9 in the positive and negative modes respectively. The molecular ions in both modes are shown in fig 5.9.



Chemical Formula: $C_{16}H_{12}ClN_2O^+$
 Exact Mass: 283.06
 Molecular Weight: 283.73

a

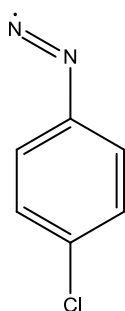


Chemical Formula: $C_{16}H_{10}ClN_2O^-$
 Exact Mass: 281.05
 Molecular Weight: 281.72

b

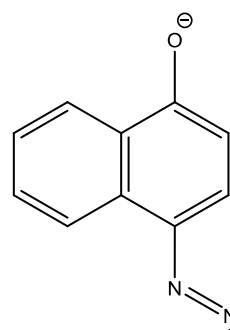
Figure 5.9 Molecular ion formed in positive (a) and negative (b) modes

Also in the negative mode, there is a peak at m/z of 298.8 which is attributed to a peak resulting from an $[M+H_2O]^-$ fragment. In addition, the peak at m/z of 171.3 is an $[X+1]^-$ can be linked to the fragment formed after the cleavage of the chloro benzene. Also the cleavage of the naphthol leads to the generation of a fragment with m/z of 138.9. These fragments are shown in fig 5.10.



Chemical Formula: $C_6H_4ClN_2^+$
 Exact Mass: 139.01

a



Chemical Formula: $C_{10}H_6N_2O^-$
 Exact Mass: 170.05

b

Figure. 5.10 Fragments with m/z of 139.0 (a) and 170.0 (b)

The ^1H NMR for this compound is very similar to that obtained for the KA 004. This is not far-fetched, seeing that the chloro group in KA 005 is at exactly the same position, *para*, as the nitro group in KA 004.

The Acetylated Products

For compound KA 006, the IR spectrum was obtained as shown in appendix F. From the spectrum, there is an absorption band at 1772.65 cm^{-1} representing the presence of a carbonyl of the acetyl group introduced. It is important to note that, the broad band at about 3200 cm^{-1} that was obtained for the starting compound, KA 004, is absent in this case.

From the IR spectrum of KA 007, appendix G, two signals can be observed at 1764.59 and 1657.15 cm^{-1} which represents the vibrations due to the two carbonyls groups present, the carboxylic acid and acetyl group. As explained earlier, the carbonyls of ester linkages (in this case the acetyl group) with higher frequencies as compared with the carboxylic acid. Therefore, the signal at 1764.59 cm^{-1} represent that of the acetyl group and that at 1657.15 cm^{-1} is that for the acid.

The Alkylated Products

From the IR spectrum, appendix H, the signal due to the $-\text{OH}$ vibration at $\sim 3200\text{ cm}^{-1}$ is not present. This signifies that the alcohol functional group has been converted into a new one, that is, the ether which is indicated by the appearance of a peak at 1210.15 cm^{-1} .

Furthermore, for the compound KA 009, appendix I, the characteristic broad band stretching over $3550 - 3200\text{ cm}^{-1}$ representing the naphthol $-\text{OH}$ cannot be observed. However the vibration of the $-\text{OH}$ of the carboxylic acid is

recorded at 2966.78 cm^{-1} . A new absorption band is also recorded at 1247.23 cm^{-1} representing the C-O-C vibrations of the ether bond formed.

5.1.3 Antimicrobial Assay

The minimum inhibitory concentration (MIC) of an antimicrobial agent can be defined as the lowest concentration of the agent needed to cause an inhibition of growth of a microorganism. The current technique of choice employed in the determination the MIC of antimicrobial agents is the broth dilution method. This method has gained grounds over the agar well diffusion because in this method, the issues of the diffusion of the test compound through the growth media is eliminated (Wiegand *et al.*, 2008).

In the dilution method, the series of the test sample contained in a nutrient broth are placed in wells on a micro-titre plate in the order of decreasing concentration, prepared through serial dilution. The microorganisms are inoculated in the wells and incubated for a period of time, mostly for 18 – 24 hours. After the incubation period, the wells are examined and the lowest concentration of the test sample that shows no microbial growth is recorded as the MIC of the sample. It is important to note that, sometimes there is the need to add a colour reagent, a tetrazolium salt, which stains the cell matter of the organism, to aid the determination of the MIC.

In this experiment, sterility and growth controls, and Cefuroxime Axetil were used as negative and positive controls respectively. In the sterility control, the organisms were inoculated with the diluting solvents without the test compounds. This gives an indication as to whether or not the solvents contribute to the inhibition. For the growth control, inoculation of the test compound and solvent without the organisms. This helps to check

contamination. Cefuroxime is a commercially available antibiotic with a general broad spectrum activity, and comparing the MIC of the synthesised dyes with this drug will provide some preliminary efficacy of dyes. The determinations were performed in duplicated in order to ensure that the results obtained were reproducible. Two gram positive organisms [(*Staphylococcus aureus* (ATCC 25923) and *Streptococcus pyrogenes* (clinical strain)], two gram negative organisms [*Salmonella typhi* (clinical strain), *Pseudomonas aeruginosa* (ATCC 4853)] and a fungus [*Candida albicans* (clinical strain)] were used in the assay. The choice of these organisms was to aid give an indication as to whether the synthesised compounds would exhibit a broad or narrow spectrum of activity.

The results obtained from the assay are summarised in table 4.2

From the results obtained, the compounds KA 001 and KA 004 showed greater activity against the fungus, *C. albicans*, recording MIC of 70.32 µg/ml and 140.63 µg/ml respectively. This is consistent with the results obtained from the work of Kofie *et al.* From that work however, an MIC of 20µg/ml was obtained for the compound KA 004 (referred to as *p*-NAαN in their work) (Kofie *et al.*, 2015). It is important to note that an ATCC 9027 strain of the organism was used in their study whereas a clinical strain sourced from the Komfo Anokye Teaching Hospital was used in this work. This may have accounted for the differences in the activities obtained.

Compound KA 002, the carboxylic acid of KA 001 is replaced by an ethyl ester group. This transformation resulted in a general increase in the activity. The ester group is less polar than the carboxylic acid, as a result, the lipophilic

character of KA 002 is improved. Hence it is able to easily move across the cell wall of the organism, to cause inhibition or death of the organism.

Also, there is the introduction of a chloro group *ortho* to the *azo* linkage of KA 004 which leads to the compound KA 003. In a study to investigate the effect of substituent and substitution pattern of the decolourization of *azo* dyes by Hsueh *et al.*, it was observed that the presence of an electron-withdrawing group *ortho* to the *azo* linkage will lead to a reduced rate of decolourization of the dye by microbes, as compared with an isomer with the substituent at the *para* position (Hsueh and Chen, 2008, Hsueh *et al.*, 2009). This observation is consistent with the results obtained from this work, in which KA 003 showed a general improvement in activity over KA 004. To explain this, steric hindrance may play a crucial role in this observed activity. Some microorganisms such as the penicillin-resistant organisms produce certain protective enzymes that adds certain groups which binds to specific positions on the antimicrobial agents which ends up inactivating the agent (Silver, 2011). In KA 003 however, binding at the chloro group will result in considerable steric problems due to the presence of the *azo* bond in the close proximity. As a result the structural integrity of the compound may be said to be intact at the site of action to cause inhibition.

In addition, the activity of KA 005 was lower than KA 004. Hsueh *et al.* demonstrated that when an electron-withdrawing group is present in a *para* position to the *azo* linkage in a dye, it is much more susceptible to microbial decolouration (Hsueh and Chen, 2008, Hsueh *et al.*, 2009). The chloro group is more electronegative than the nitro group as a result will exhibit a higher electron-withdrawing effect, hence the susceptibility to microbial degradation

will be higher than that of the nitro dye. This explains the reduced activity of KA 005 compared with KA 004.

Furthermore, from the microbial testing of the alkylated products, KA 008 and KA 009, it was revealed that presence of the ether group contributed significantly in improving the activity of these compounds. These results are not far-fetched, considering that the ether compound is less polar than the base phenolic compound. This reduced polarity increases the lipophilicity of these compounds therefore making them easy to transport across the cell wall of the microorganism to cause death or inhibition of growth.

This same improvement in the activity was expected for the acetylated products, KA 006 and KA 007, since they are also more non-polar. However, from the study, a rather decrease in activity was obtained instead. The acetylated products are about 42 units heavier than their base compound. This extra weight may have contributed in slowing down the rate of diffusion of the compounds across the cell walls of the organisms to cause inhibition, hence the lower MIC.

Finally, the commercially available antibiotic, cefuroxime axetil, was used as the positive control in this work. The most active synthesised compound, KA 008, recorded some comparable activities against some of the organisms used as the control drug, 35.16 $\mu\text{g/ml}$ against *S. pyrogenes* and *P. aeruginosa* for both KA 008 and the control. This goes to show that this compound has great potential to be used as an antimicrobial agent.

In spite of this great promise, before any claims can be made, there is the need for *in vivo* and toxicity studies to ascertain the efficacy and safety of this compound in living cells.

5.2 CONCLUSION

In summary, nine *azo* compounds have been successfully synthesised, and in good yields. Using the standard direct *diazotization-coupling* procedure, five compounds were synthesised. The Williamson's ether synthesis as well as the acetylation with acetic anhydride were also used to synthesize the alkylated and acetylated products respectively. The compounds have been partially characterised.

All the synthesised dyes showed antimicrobial activity, generally showing more activity against the gram negative and fungus.

Generally, the introduction of electron-withdrawing groups *ortho* to the *azo* linkage, results in an increase in the activity of the compound through the introduction of steric issues, as seen in the activity of KA 003. Also, alkylation of the hydroxyl of the naphthol leads to the improvement in the lipid solubility profile of the products hence an increase in the activity of the alkylated derivatives. The structures of the most active compounds are shown in fig. 5.11.

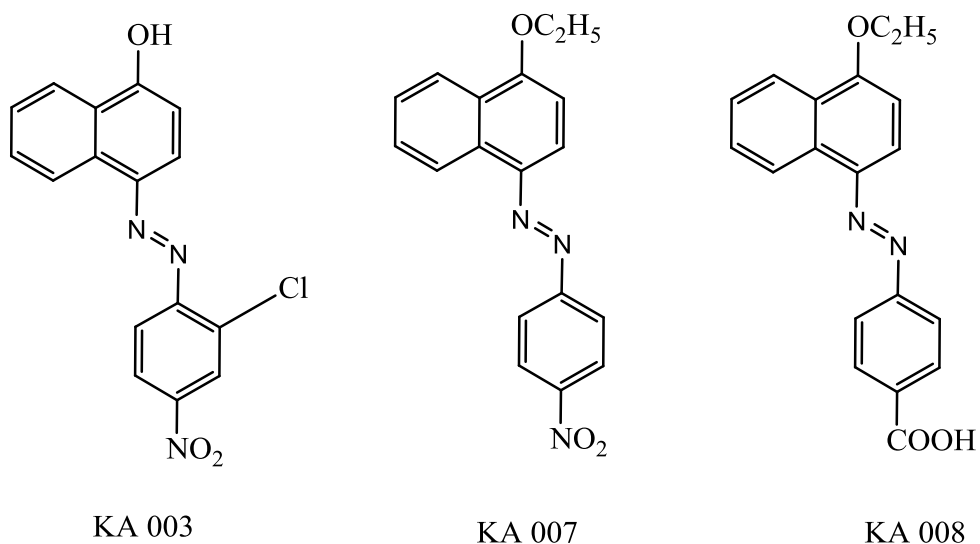


Figure 5.11 Structures of the most active synthesised dyes

Also, the most active compound, KA 008, showed comparable activities with the standard Cefuroxime axetil used, indicating it's potential to be used as an antimicrobial agent.

5.3 RECOMMENDATION

- Further structural modification by the increasing of the carbon chain in the ether and ester derivatives can be explored. This will help to show whether or not increasing the carbon chain of these derivatives would improve activity.
- Toxicity studies should be conducted to ascertain the safety profile of the active compound. Compound KA 008 showed comparable activity as the standard cefuroxime, hence if should be developed as an antimicrobial agent, its safety should be assured.

REFERENCES

- ANDRIOLE, V. T. 2005. The quinolones: past, present, and future. *Clinical Infectious Diseases*, 41, S113-S119.
- AVCI, G. A., OZKINALI, S., OZLUK, A., AVCI, E. & KOCAOKUTGEN, H. 2012. Antimicrobial activities, absorption characteristics and tautomeric structures of o, o'-hydroxyazo dyes containing an acryloyloxy group and their chromium complexes. *Hacettepe J. Biol. Chem*, 40, 119-26.
- BAFANA, A., DEVI, S. S. & CHAKRABARTI, T. 2011. Azo dyes: past, present and the future. *Environmental Reviews*, 19, 350-371.
- BO, G. 2000. Giuseppe Brotzu and the discovery of cephalosporins. *Clinical microbiology and infection*, 6, 6-8.
- CHUNG, K.-T., CHEN, S.-C., WONG, T. Y., LI, Y.-S., WEI, C.-I. & CHOU, M. W. 2000. Mutagenicity studies of benzidine and its analogs: structure-activity relationships. *Toxicological Sciences*, 56, 351-356.
- CHUNG, K.-T., STEVENS, S. E. & CERNIGLIA, C. E. 2008. The reduction of azo dyes by the intestinal microflora. *Critical reviews in microbiology*.
- FLEMING, A. 1946. Penicillin. Its practical application. *Penicillin. Its practical application*.
- GARFIELD, S. 2002. *Mauve: how one man invented a color that changed the world*, WW Norton & Company.
- GARJANI, A., DAVARAN, S., RASHIDI, M. & MALEK, N. 2004. Protective effects of some azo derivatives of 5-aminosalicylic acid and their pegylated prodrugs on acetic acid-induced rat colitis. *DARU Journal of Pharmaceutical Sciences*, 12, 24-30.
- GOLD, V., LOENING, K., MCNAUGHT, A. & SHEMI, P. 1997. IUPAC Compendium of Chemical Terminology. *Blackwell Science, Oxford*.

- GORDON, P. F. & GREGORY, P. 2012. *Organic chemistry in colour*, Springer Science & Business Media.
- HARADA, T., YABUKI, Y., OGAWA, M. & IWANAGA, H. 2005. Ink, ink jet recording method and azo compound. Google Patents.
- HAYASHI, K., TAKAHATA, M., KAWAMURA, Y. & TODO, Y. 2001. Synthesis, antibacterial activity, and toxicity of 7-(isoindolin-5-yl)-4-oxoquinoline-3-carboxylic acids. Discovery of the novel des-F (6)-quinolone antibacterial agent garenoxacin (T-3811 or BMS-284756). *Arzneimittel-Forschung*, 52, 903-913.
- HSUEH, C.-C. & CHEN, B.-Y. 2008. Exploring effects of chemical structure on azo dye decolorization characteristics by *Pseudomonas luteola*. *Journal of Hazardous Materials*, 154, 703-710.
- HSUEH, C.-C., CHEN, B.-Y. & YEN, C.-Y. 2009. Understanding effects of chemical structure on azo dye decolorization characteristics by *Aeromonas hydrophila*. *Journal of hazardous materials*, 167, 995-1001.
- ISPIR, E. 2009. The synthesis, characterization, electrochemical character, catalytic and antimicrobial activity of novel, azo-containing Schiff bases and their metal complexes. *Dyes and Pigments*, 82, 13-19.
- KEERTHI KUMAR, C. T., KESHAVAYYA, J., RAJESH, T. N., PEETHAMBAR, S. K. & SHOUKAT ALI, A. R. 2013. Synthesis, Characterization, and Biological Activity of 5-Phenyl-1, 3, 4-thiadiazole-2-amine Incorporated Azo Dye Derivatives. *Organic Chemistry International*, 2013.
- KOFIE, W., DZIDZOR, A. C. & ADOSRAKU, R. K. 2015. Synthesis and Evaluation of Antimicrobial Properties of Azo Dyes. *International Journal of Pharmacy and Pharmaceutical Sciences*, 7.
- LOWY, F. D. 2003. Antimicrobial resistance: the example of *Staphylococcus aureus*. *The Journal of Clinical Investigation*, 111, 1265-1273.

- MAKENA, P. S. & CHUNG, K.-T. 2007. Effects of various plant polyphenols on bladder carcinogen benzidine-induced mutagenicity. *Food and Chemical Toxicology*, 45, 1899-1909.
- MAVROVA, A. T., WESSELINOVA, D., TSENOV, Y. A. & DENKOVA, P. 2009. Synthesis, cytotoxicity and effects of some 1, 2, 4-triazole and 1, 3, 4-thiadiazole derivatives on immunocompetent cells. *European journal of medicinal chemistry*, 44, 63-69.
- MORRIS, P. J. & TRAVIS, A. S. 1992. A history of the international dyestuff industry. *American Dyestuff Reporter*, 81, 59-59.
- NATANSOHN, A. & ROCHON, P. 2002. Photoinduced motions in azo-containing polymers. *Chemical Reviews*, 102, 4139-4176.
- NEU, H. C. 1992. The crisis in antibiotic resistance. *Science*, 257, 1064-1073.
- ONO, M., WADA, Y., WU, Y., NEMORI, R., JINBO, Y., WANG, H., LO, K.-M., YAMAGUCHI, N., BRUNKHORST, B., OTOMO, H., WESOLOWSKI, J., WAY, J. C., ITOH, I., GILLIES, S. & CHEN, L. B. 1997. FP-21399 blocks HIV envelope protein-mediated membrane fusion and concentrates in lymph nodes. *Nat Biotech*, 15, 343-348.
- PANDEY, A., SINGH, P. & IYENGAR, L. 2007. Bacterial decolorization and degradation of azo dyes. *International Biodeterioration & Biodegradation*, 59, 73-84.
- RASHEED, O. K. 2011. *New directions in the chemistry of azo-compounds*. University of Manchester.
- REGITZ, M. 2012. *Diazo compounds: properties and synthesis*, Elsevier.
- ROCA, I., AKOVA, M., BAQUERO, F., CARLET, J., CAVALERI, M., COENEN, S., COHEN, J., FINDLAY, D., GYSSENS, I., HEURE, O. E., KAHLMETER, G., KRUSE, H., LAXMINARAYAN, R., LIEBANA, E., LOPEZ-CERERO, L., MACGOWAN, A., MARTINS, M., RODRIGUEZ-BANO, J., ROLAIN, J. M., SEGOVIA, C., SIGAUQUE, B., TACONELLI, E., WELLINGTON, E. & VILA, J.

2015. The global threat of antimicrobial resistance: science for intervention. *New Microbes New Infect*, 6, 22-9.
- SHRIDHAR, A., KESHAVAYYA, J., HOSKERI, H. J. & ALI, R. S. 2011. Synthesis of some novel bis 1, 3, 4-oxadiazole fused azo dye derivatives as potent antimicrobial agents. *International Research Journal of Pure and Applied Chemistry*, 1, 119.
- SILVER, L. L. 2011. Challenges of antibacterial discovery. *Clinical microbiology reviews*, 24, 71-109.
- SOLOMONS, T. W. G., FRYHLE, C.B. 2012. *Organic Chemistry*, Wiley.
- SPONZA, D. T. & IŞIK, M. 2005. Reactor performances and fate of aromatic amines through decolorization of Direct Black 38 dye under anaerobic/aerobic sequential. *Process biochemistry*, 40, 35-44.
- STELLBRINK, H.-J. 2007. Antiviral drugs in the treatment of AIDS: what is in the pipeline? *European journal of medical research*, 12, 483-495.
- SWATI, G., ROMILA, K., SHARMA, I. & VERMA, P. 2011. Synthesis, characterisation and antimicrobial screening of some azo compounds. *International Journal of Applied Biology and Pharmaceutical Technology*, 2, 332-338.
- SYKES, R. & BONNER, D. 1985. Discovery and development of the monobactams. *Review of Infectious Diseases*, 7, S579-S593.
- TURSI, A., BRANDIMARTE, G., GIORGETTI, G. M., FORTI, G., MODEO, M. E. & GIGLIOBIANCO, A. 2004. Low-dose balsalazide plus a high-potency probiotic preparation is more effective than balsalazide alone or mesalazine in the treatment of acute mild-to-moderate ulcerative colitis. *Medical Science Monitor Basic Research*, 10, PI126-PI131.
- WAINWRIGHT, M. 2008. Dyes in the development of drugs and pharmaceuticals. *Dyes and Pigments*, 76, 582-589.
- WAINWRIGHT, M. & KRISTIANSEN, J. E. 2011. On the 75th anniversary of Prontosil. *Dyes and Pigments*, 88, 231-234.

WHO 2014. ANTIMICROBIAL RESISTANCE: Global Report on Surveillance.

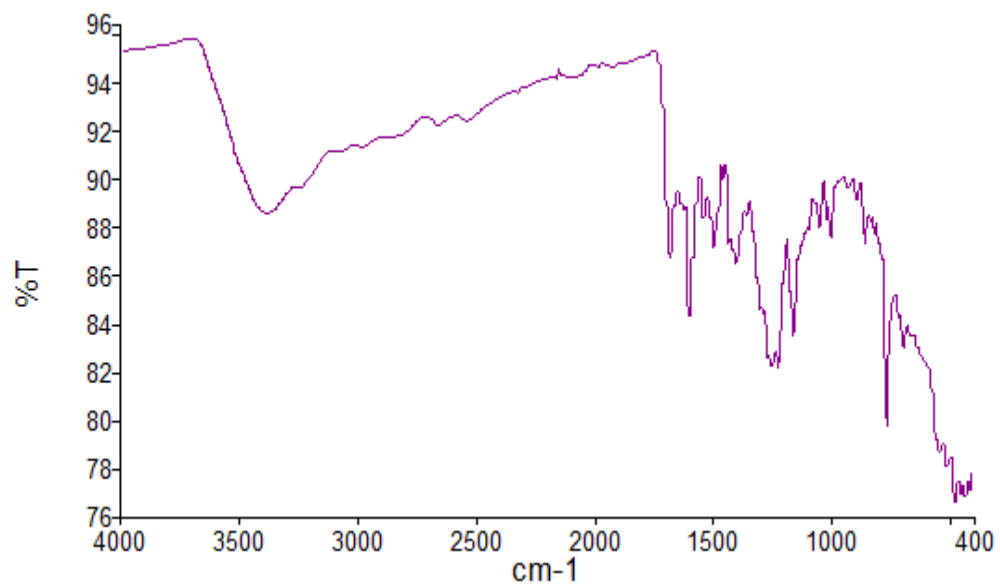
WIEGAND, I., HILPERT, K. & HANCOCK, R. E. 2008. Agar and broth dilution methods to determine the minimal inhibitory concentration (MIC) of antimicrobial substances. *Nature protocols*, 3, 163-175.

YAROSHCHUK, O. & REZNIKOV, Y. 2012. Photoalignment of liquid crystals: basics and current trends. *Journal of Materials Chemistry*, 22, 286-300.

APPENDICES

Appendix A; Analytical Data for KA 001

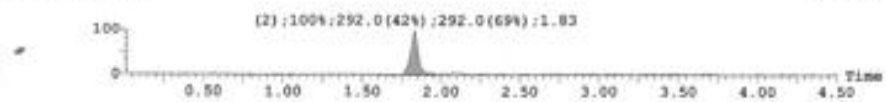
(1) IR Spectrum



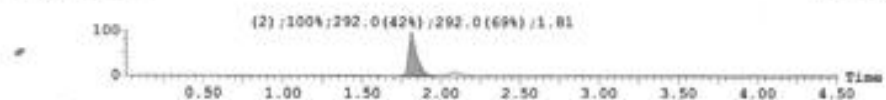
(2) Mass Spec

Printed: Fri Jan 08 12:43:38 2016

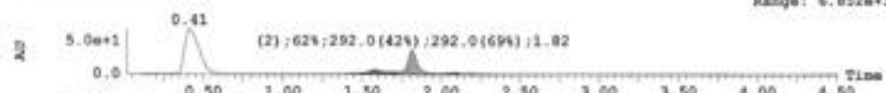
1: MS ES+ :293 1.4e+006



2: MS ES- :291 1.4e+006

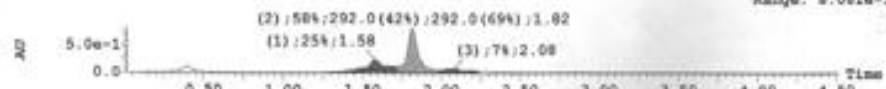


3: UV Detector: TIC 6.852e+1
Range: 6.852e+1



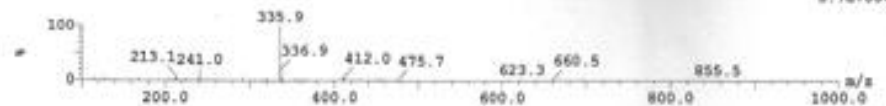
| Peak Number | Mass Found | Time | Area %Total |
|-------------|----------------|------|-------------|
| 1 | | 1.58 | 25.33 |
| 2 | 292.00, 292.00 | 1.82 | 62.28 |
| 3 | | 2.09 | 7.57 |
| 4 | | 2.19 | 2.81 |
| 5 | | 2.26 | 2.00 |

3: UV Detector: 252_256 8.081e-1
Range: 8.081e-1



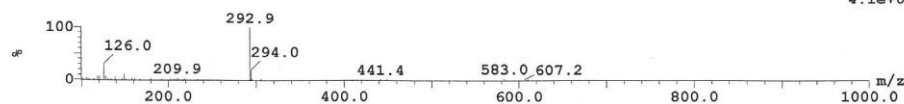
| Peak Number | Mass Found | Time | Area %Total |
|-------------|----------------|------|-------------|
| 1 | | 1.58 | 24.73 |
| 1 | | 1.67 | 7.25 |
| 2 | 292.00, 292.00 | 1.82 | 57.89 |
| 3 | | 2.08 | 7.47 |
| 4 | | 2.19 | 2.67 |

1: (Time: 1.58) Combine (41:45-(30:32+32:55)) 2: MS ES- 8.7e+004

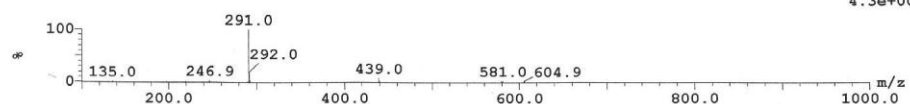


Printed: Fri Jan 08 12:43:38 2016

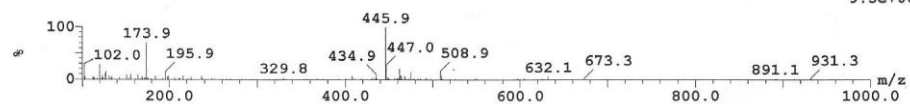
2: (Time: 1.83) Combine (49:53-(43:44+59:62)) 1: MS ES+
4.1e+005



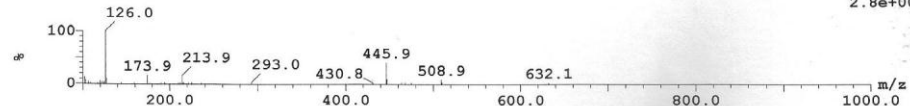
2: (Time: 1.81) Combine (48:52-(43:44+58:61)) 2: MS ES-
4.3e+005



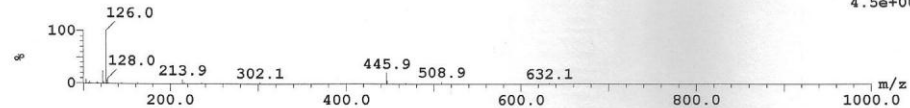
3: (Time: 2.09) Combine (56:60-(50:51+64:67)) 1: MS ES+
9.5e+004



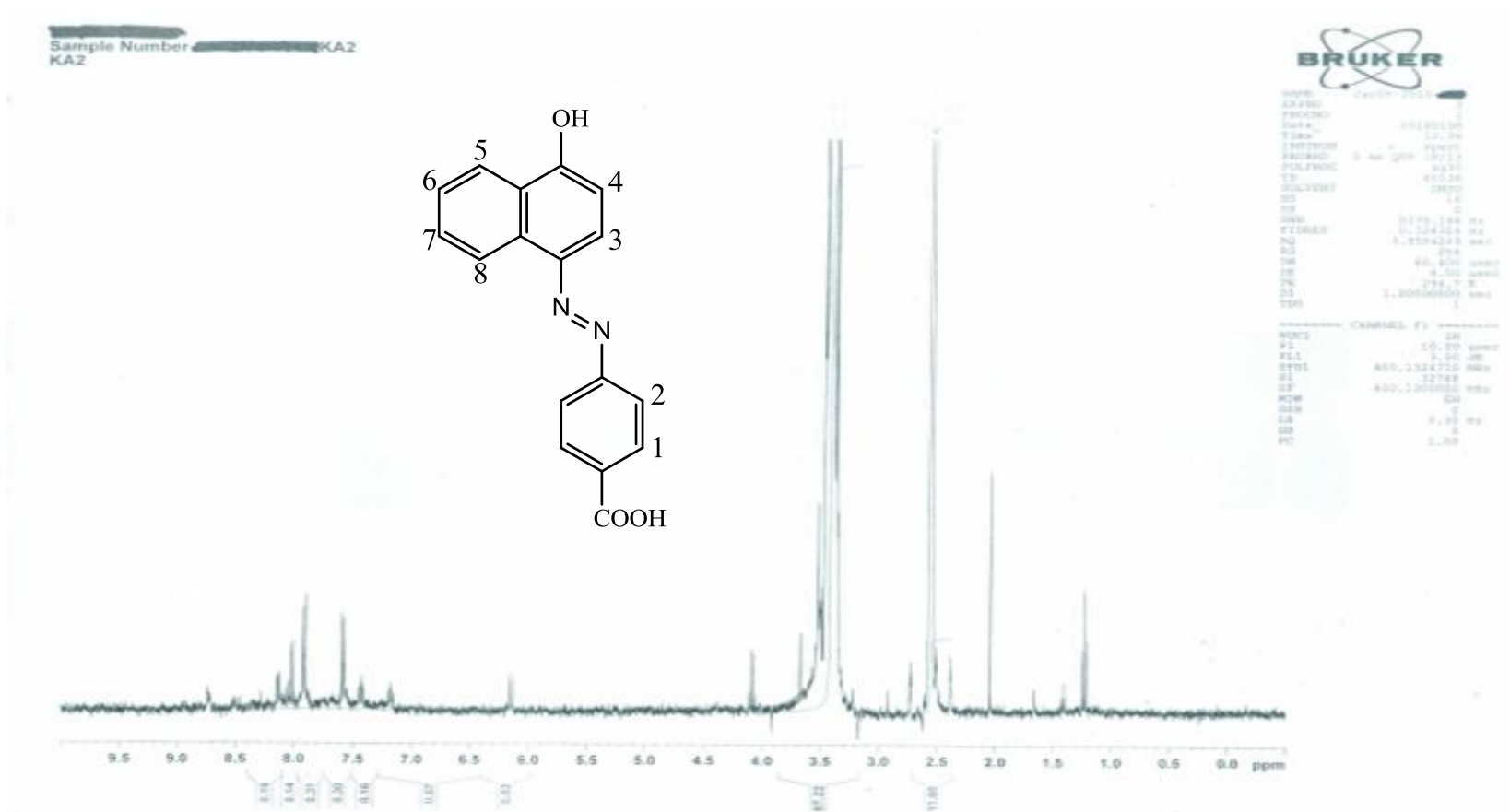
4: (Time: 2.19) Combine (58:62-(54:56+66:69)) 1: MS ES+
2.8e+005



5: (Time: 2.26) Combine (60:64-(57:58+74:77)) 1: MS ES+
4.5e+005

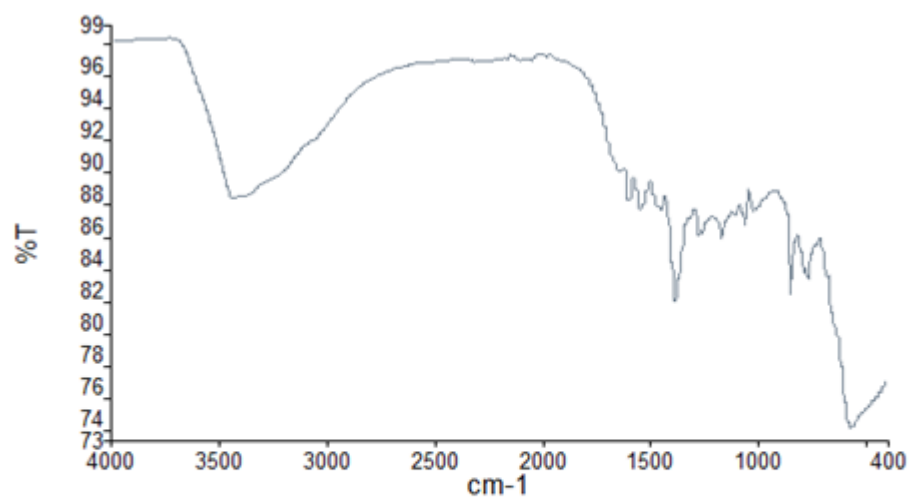


(3) ^1H NMR



Appendix B; Analytical Data for KA 002

(1) IR Spectrum



| Name | Description |
|---------------------|-------------|
| —Kwaku Addo-Danquah | KA 002 |

Peak Table

| Peak | X | Y | Peak | X | Y | Peak | X | Y | Peak | X | Y |
|------|---------|-------|------|---------|-------|------|---------|-------|------|--------|-------|
| 1 | 3376.82 | 88.73 | 2 | 1380.25 | 82 | 3 | 1169.33 | 85.97 | 4 | 846.66 | 82.46 |
| 5 | 762.54 | 83.5 | 6 | 558.91 | 74.05 | | | | | | |

(2) Mass Spec

Openlynx [REDACTED] OA3 LCMS Generic Chromatography [REDACTED] Page 3

File: OA3_160108_013

ID: KA2

Description:

Vial: 3:3

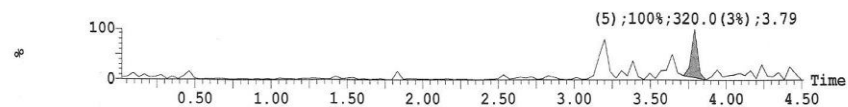
Date: 08-Jan-2016

Time: 12:30:43

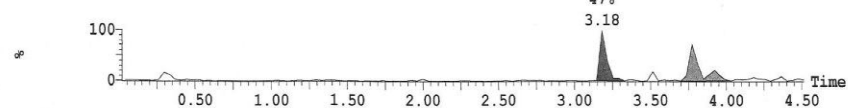
Submitter:

Printed: Fri Jan 08 12:43:38 2016

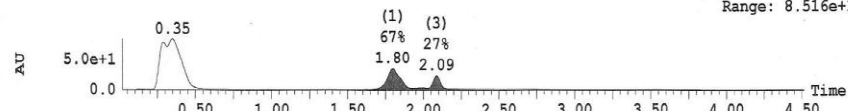
1: MS ES+ :321 3.3e+004



2: MS ES- :319 5.2e+004

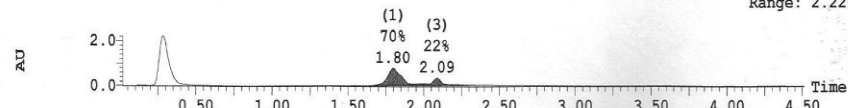


3: UV Detector: TIC 8.517e+1
Range: 8.516e+1



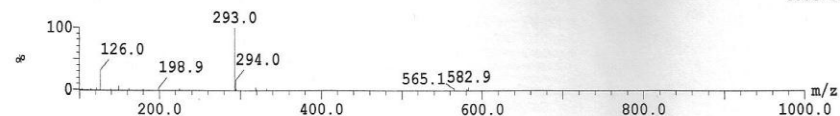
| Peak Number | Mass Found | Time | Area %Total |
|-------------|------------|------|-------------|
| 1 | | 1.80 | 67.24 |
| 2 | | 1.99 | 5.38 |
| 3 | | 2.09 | 27.38 |

3: UV Detector: 252_256 2.226
Range: 2.226

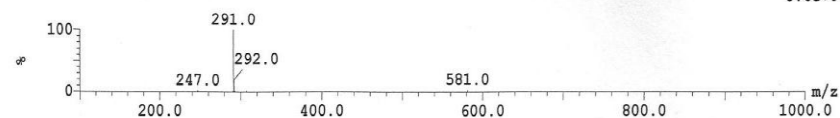


| Peak Number | Mass Found | Time | Area %Total |
|-------------|------------|------|-------------|
| 1 | | 1.80 | 70.38 |
| 2 | | 1.99 | 7.18 |
| 3 | | 2.09 | 22.44 |

1: (Time: 1.80) Combine (48:52-(39:40+58:61)) 1: MS ES+
6.0e+005



1: (Time: 1.80) Combine (47:51-(38:40+58:60)) 2: MS ES-
8.6e+005



File: OA3_160108_013

ID: KA2

Description:

Vial: 3:3

Date: 08-Jan-2016

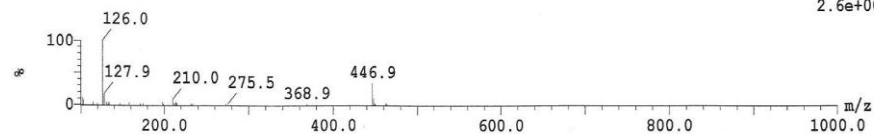
Time: 12:30:43

Submitter:

Printed: Fri Jan 08 12:43:38 2016

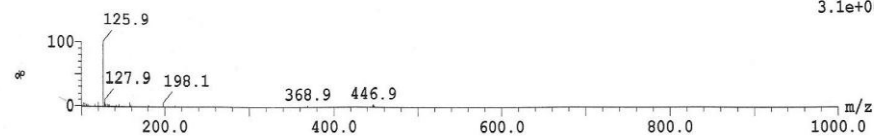
2: (Time: 1.99) Combine (53:57-(49:50+61:63))

1: MS ES+
2.6e+005



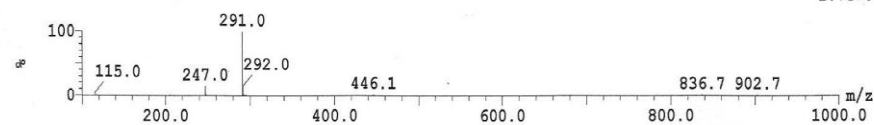
3: (Time: 2.09) Combine (56:60-(51:53+70:73))

1: MS ES+
3.1e+005



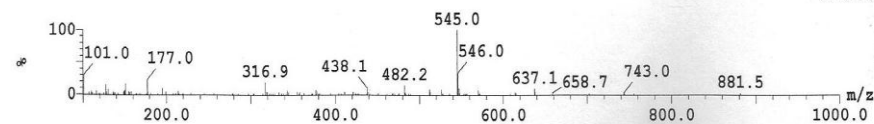
3: (Time: 2.09) Combine (55:59-(51:52+70:73))

2: MS ES-
1.7e+005



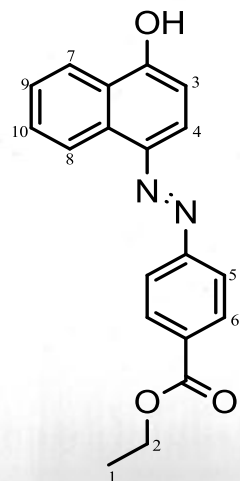
5: (Time: 3.79) Combine (102:106-(97:98+110:113))

1: MS ES+
2.6e+005

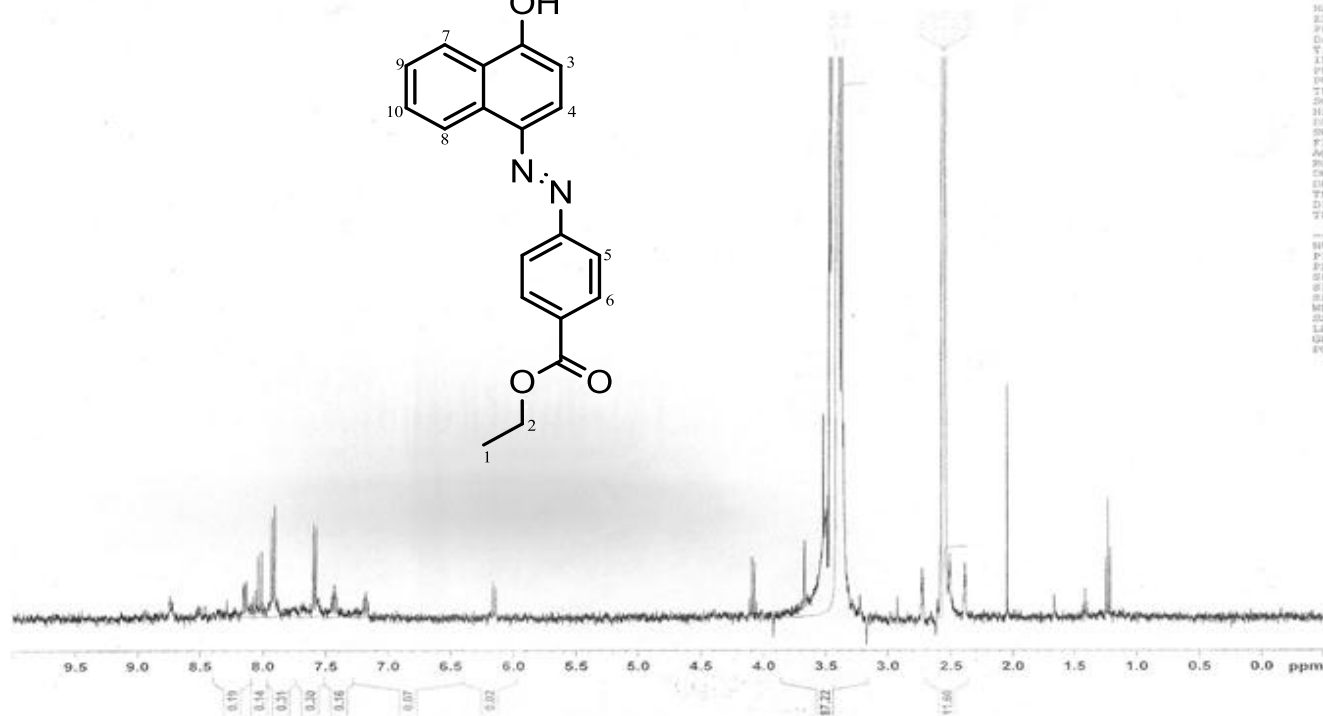


(3) ¹H NMR

Sample Number KA2

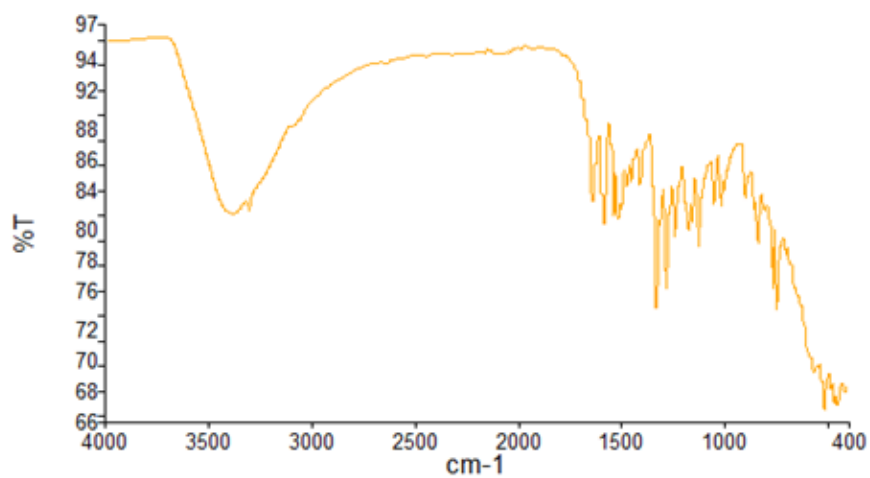


```
NAME: Jach-2010
EXNO: 1
PROCNO: 1
Date_: 20160108
Time: 12.36
INSTRUM: spect
PROBHD: 5 mm ZNP CHV13
PULPROG: zgpg30
TD: 65536
SOLVENT: DMSO
NS: 1632
DS: 4
SWH: 8278.144 Hz
FIDRES: 0.126324 Hz
AQ: 3.9584243 sec
RG: 256
SN: 60,400
DE: 6.00 um
TE: 294.1 K
D1: 1.60000000 sec
TD0: 1
----- CHANNEL f1 -----
NUC1: 1H
P1: 10.00 usec
PL1: 3.00 dB
SFO1: 400.1324110 MHz
SI: 32768
SF: 400.1320000 MHz
WDW: EM
SSB: 0
LB: 0.30 Hz
GB: 0
PC: 1.00
```



Appendix C; Analytical Data for KA 003

(1) IR Spectrum



| Name | Description |
|----------------------|-------------|
| — Kwaku Addo-Danquah | KA 003 |

Peak Table

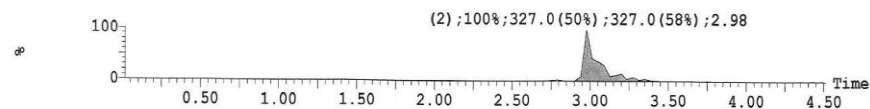
| Peak | X | Y |
|------|---------|-------|------|---------|-------|------|---------|-------|------|---------|-------|
| 1 | 3378.14 | 82.36 | 2 | 1637.35 | 83.37 | 3 | 1584.75 | 81.33 | 4 | 1538.05 | 82.05 |
| 5 | 1512.76 | 81.74 | 6 | 1406.79 | 84.6 | 7 | 1329.22 | 74.51 | 8 | 1302.43 | 81.2 |
| 9 | 1276.23 | 76.2 | 10 | 1242.36 | 80.29 | 11 | 1168.6 | 80.83 | 12 | 1118.77 | 79.56 |
| 13 | 1047.37 | 83.07 | 14 | 1011.07 | 82.94 | 15 | 894.74 | 83.57 | 16 | 832.43 | 79.84 |
| 17 | 761.67 | 78.17 | 18 | 742.77 | 74.46 | 19 | 514.81 | 66.32 | 20 | 447.63 | 66.62 |

(2) Mass Spec

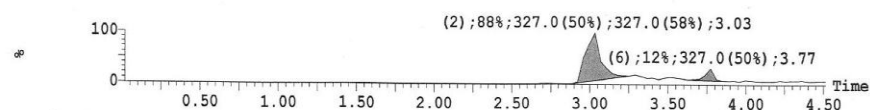
Openlynx [REDACTED]_OA3 LCMS Generic Chromatography. [REDACTED] Page 5
 File:OA3_160108_014 ID:KA3 Description:
 Vial:3:4 Date:08-Jan-2016 Time:12:37:08
 Submitter:

Printed: Fri Jan 08 12:43:38 2016

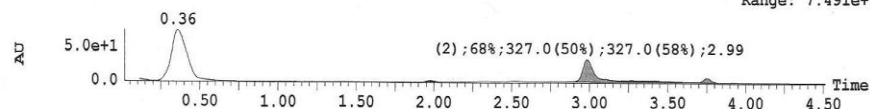
1: MS ES+ :328 3.7e+006



2: MS ES- :326 5.9e+006

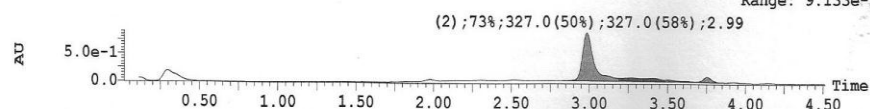


3: UV Detector: TIC 7.491e+1
Range: 7.491e+1



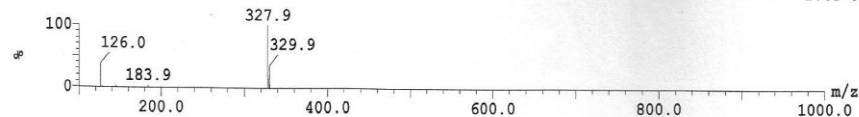
| Peak Number | Mass Found | Time | Area %Total |
|-------------|----------------|------|-------------|
| 1 | | 1.98 | 3.41 |
| 2 | 327.00, 327.00 | 2.99 | 67.77 |
| 3 | | 3.27 | 9.08 |
| 4 | | 3.42 | 10.23 |
| 6 | 327.00 | 3.75 | 9.51 |

3: UV Detector: 252_256 9.133e-1
Range: 9.133e-1



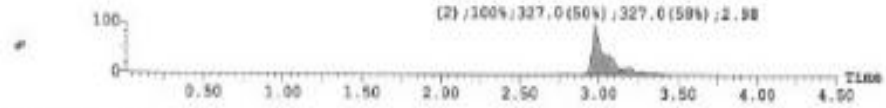
| Peak Number | Mass Found | Time | Area %Total |
|-------------|----------------|------|-------------|
| 2 | 327.00, 327.00 | 2.99 | 72.67 |
| 3 | | 3.27 | 9.61 |
| 4 | | 3.40 | 7.22 |
| 5 | | 3.51 | 4.49 |
| 6 | 327.00 | 3.75 | 6.01 |

2:(Time: 2.98) Combine (80:84-(74:75+100:103)) 1:MS ES+
1.6e+006

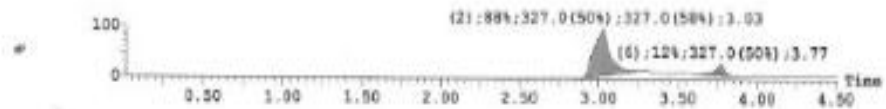


Printed: Fri Jan 08 12:43:38 2016

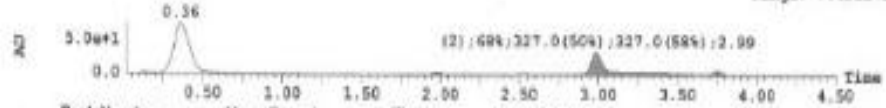
1: MS ES+ :328 3.7e+006



2: MS ES- :324 5.9e+006

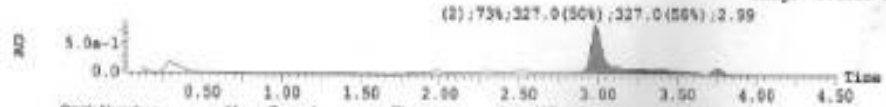


3: UV Detector: TIC 7.491e+1
Range: 7.491e+1



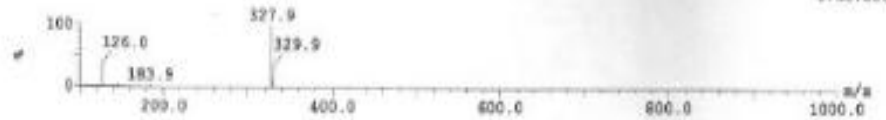
| Peak Number | Mass Found | Time | Area %Total |
|-------------|----------------|------|-------------|
| 1 | | 1.98 | 3.41 |
| 2 | 327.00, 327.00 | 2.99 | 67.77 |
| 3 | | 3.27 | 9.09 |
| 4 | | 3.42 | 10.23 |
| 6 | 327.00 | 3.75 | 9.51 |

3: UV Detector: 252_256 9.133e-1
Range: 9.133e-1



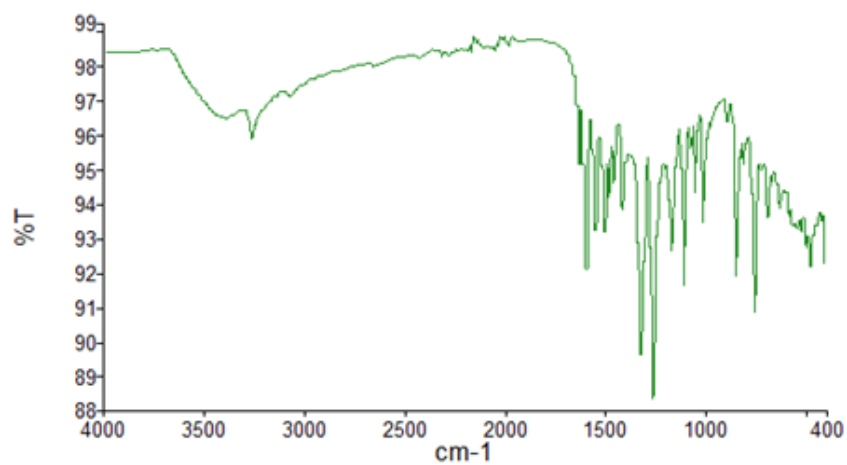
| Peak Number | Mass Found | Time | Area %Total |
|-------------|----------------|------|-------------|
| 2 | 327.00, 327.00 | 2.99 | 72.67 |
| 3 | | 3.27 | 0.61 |
| 4 | | 3.40 | 7.22 |
| 5 | | 3.51 | 4.43 |
| 6 | 327.00 | 3.75 | 6.01 |

2: (Time: 2.98) Combine (80:84-(74:75+100:103)) 1: MS ES+
1.6e+006



Appendix D; Analytical Data for KA 004

(1) IR Spectrum



| Name | Description |
|--------------------|-------------|
| Kwaku Addo-Danquah | KA 004 |

Peak Table

| Peak | X | Y |
|------|---------|-------|------|---------|-------|------|---------|-------|------|---------|-------|
| 1 | 3267.1 | 95.99 | 2 | 1594.29 | 92.1 | 3 | 1547.51 | 93.27 | 4 | 1502.28 | 93.24 |
| 5 | 1319.45 | 89.59 | 6 | 1258.74 | 88.3 | 7 | 1187.5 | 92.69 | 8 | 1107.99 | 91.68 |
| 9 | 1046.99 | 94.39 | 10 | 1013.34 | 93.48 | 11 | 847.59 | 91.95 | 12 | 750.48 | 90.83 |

(2) Mass Spec

Openlynx: [REDACTED] OA3 LCMS Generic Chromatography. [REDACTED] Page 1

File: OA3_160108_015

ID: KA4

Description:

Vial: 3:5

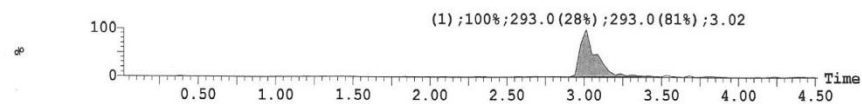
Date: 08-Jan-2016

Time: 12:43:31

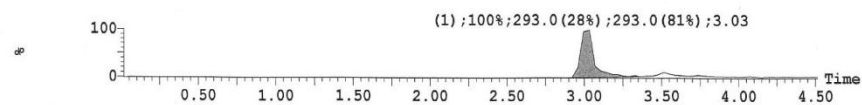
Submitter:

Printed: Fri Jan 08 13:03:10 2016

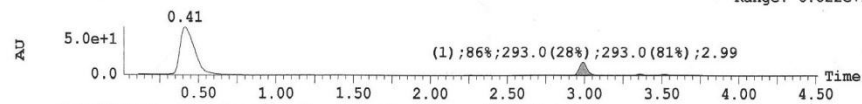
1: MS ES+ :294 7.5e+005



2: MS ES- :292 6.4e+006

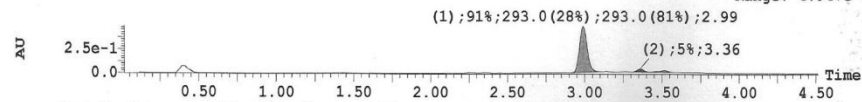


3: UV Detector: TIC 6.822e+1
Range: 6.822e+1



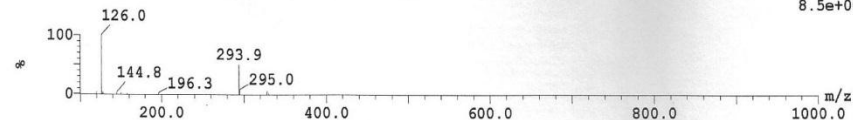
| Peak Number | Mass Found | Time | Area %Total |
|-------------|----------------|------|-------------|
| 1 | 293.00, 293.00 | 2.99 | 86.35 |
| 2 | | 3.36 | 6.45 |
| 3 | 293.00 | 3.52 | 7.20 |

3: UV Detector: 252_256 4.947e-1
Range: 4.947e-1

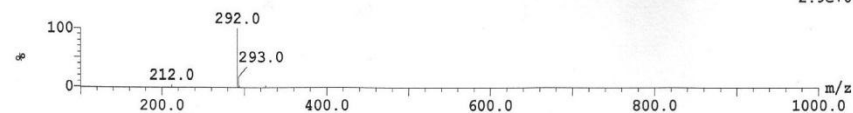


| Peak Number | Mass Found | Time | Area %Total |
|-------------|----------------|------|-------------|
| 1 | 293.00, 293.00 | 2.99 | 90.59 |
| 2 | | 3.36 | 5.35 |
| 3 | 293.00 | 3.52 | 4.06 |

1: (Time: 3.02) Combine (81:85-(75:76+99:102)) 1:MS ES+
8.5e+005

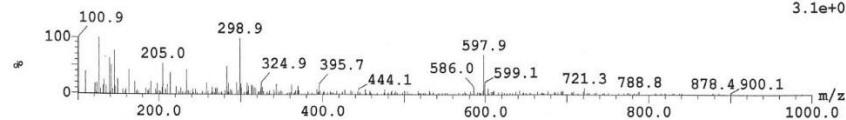


1: (Time: 3.03) Combine (81:85-(74:75+96:99)) 2:MS ES-
2.9e+006

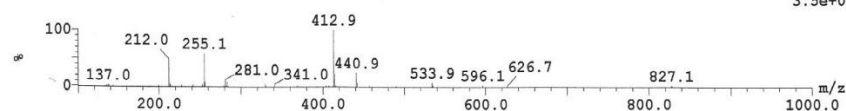


Printed: Fri Jan 08 13:03:10 2016

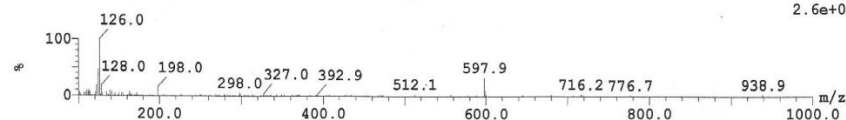
2: (Time: 3.36) Combine (90:94-(86:87+98:101)) 1:MS ES+
3.1e+004



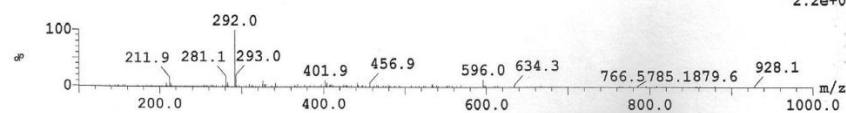
2: (Time: 3.36) Combine (89:94-(85:87+98:101)) 2:MS ES-
3.5e+005



3: (Time: 3.52) Combine (94:98-(89:90+104:107)) 1:MS ES+
2.6e+005

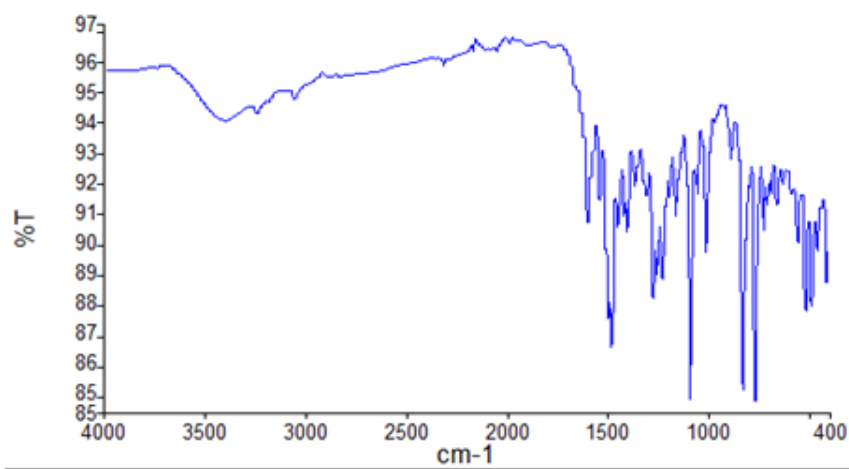


3: (Time: 3.52) Combine (94:98-(88:90+103:106)) 2:MS ES-
2.2e+005



Appendix E; Analytical Data for KA 005

(1) IR Spectrum



| Name | Description |
|--------------------|-------------|
| Kwaku Addo-Danquah | KA 005 |

Peak Table

| Peak | X | Y |
|------|---------|-------|------|---------|-------|------|---------|-------|------|---------|-------|
| 1 | 1596.69 | 90.82 | 2 | 1479.22 | 86.63 | 3 | 1404.11 | 90.43 | 4 | 1272.28 | 88.25 |
| 5 | 1155.61 | 90.97 | 6 | 1088.97 | 84.93 | 7 | 1008.34 | 89.79 | 8 | 824.05 | 85.15 |
| 9 | 763.76 | 84.82 | 10 | 727.4 | 90.5 | 11 | 511.48 | 87.8 | 12 | 484.51 | 87.95 |

(2) Mass Spec

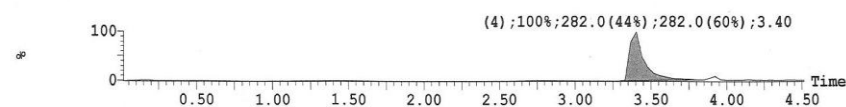
Openlynx [REDACTED] OA3 LCMS Generic Chromatography. [REDACTED] Page 3
 File: OA3_160108_016 ID: KA5 Description:
 Vial: 3:6 Date: 08-Jan-2016 Time: 12:50:21
 Submitter:

Printed: Fri Jan 08 13:03:10 2016

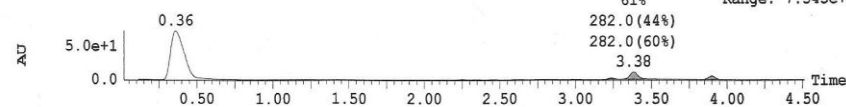
1: MS ES+ :283 3.5e+006



2: MS ES- :281 8.0e+006



3: UV Detector: TIC (4) 7.345e+1



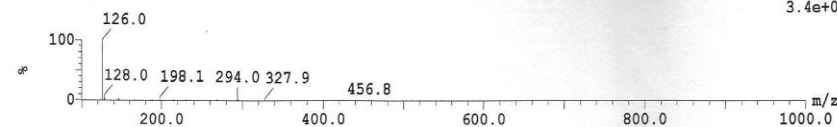
| Peak Number | Mass Found | Time | Area %Total |
|-------------|----------------|------|-------------|
| 1 | | 2.25 | 1.65 |
| 2 | | 3.00 | 2.43 |
| 3 | | 3.24 | 11.93 |
| 4 | 282.00, 282.00 | 3.38 | 61.03 |
| 6 | 282.00 | 3.90 | 22.97 |

3: UV Detector: 252_256 2.869e-1



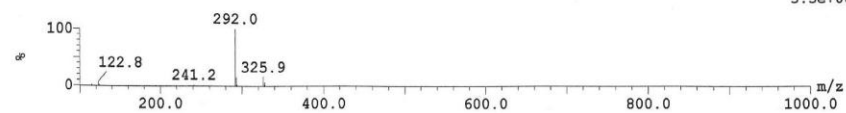
| Peak Number | Mass Found | Time | Area %Total |
|-------------|----------------|------|-------------|
| 2 | | 3.00 | 3.42 |
| 3 | | 3.24 | 13.32 |
| 4 | 282.00, 282.00 | 3.38 | 62.97 |
| 5 | | 3.81 | 3.40 |
| 6 | 282.00 | 3.90 | 16.88 |

2: (Time: 3.00) Combine (80:84-(76:77+89:92)) 1: MS ES+ 3.4e+005

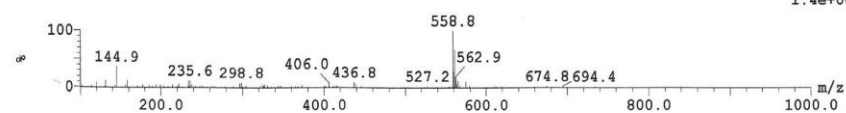


Printed: Fri Jan 08 13:03:10 2016

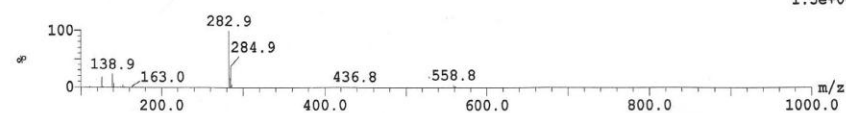
2: (Time: 3.00) Combine (80:84-(75:77+88:91)) 2:MS ES-
3.5e+005



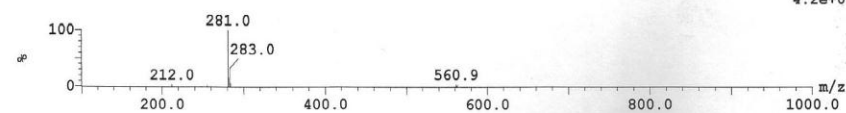
3: (Time: 3.24) Combine (87:91-(82:83+95:97)) 1:MS ES+
1.4e+005



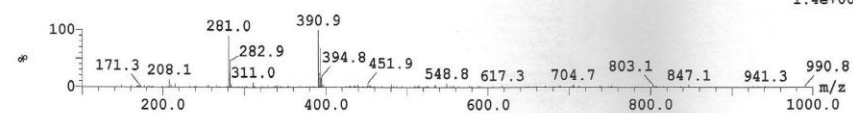
4: (Time: 3.39) Combine (91:95-(84:85+109:112)) 1:MS ES+
1.5e+006



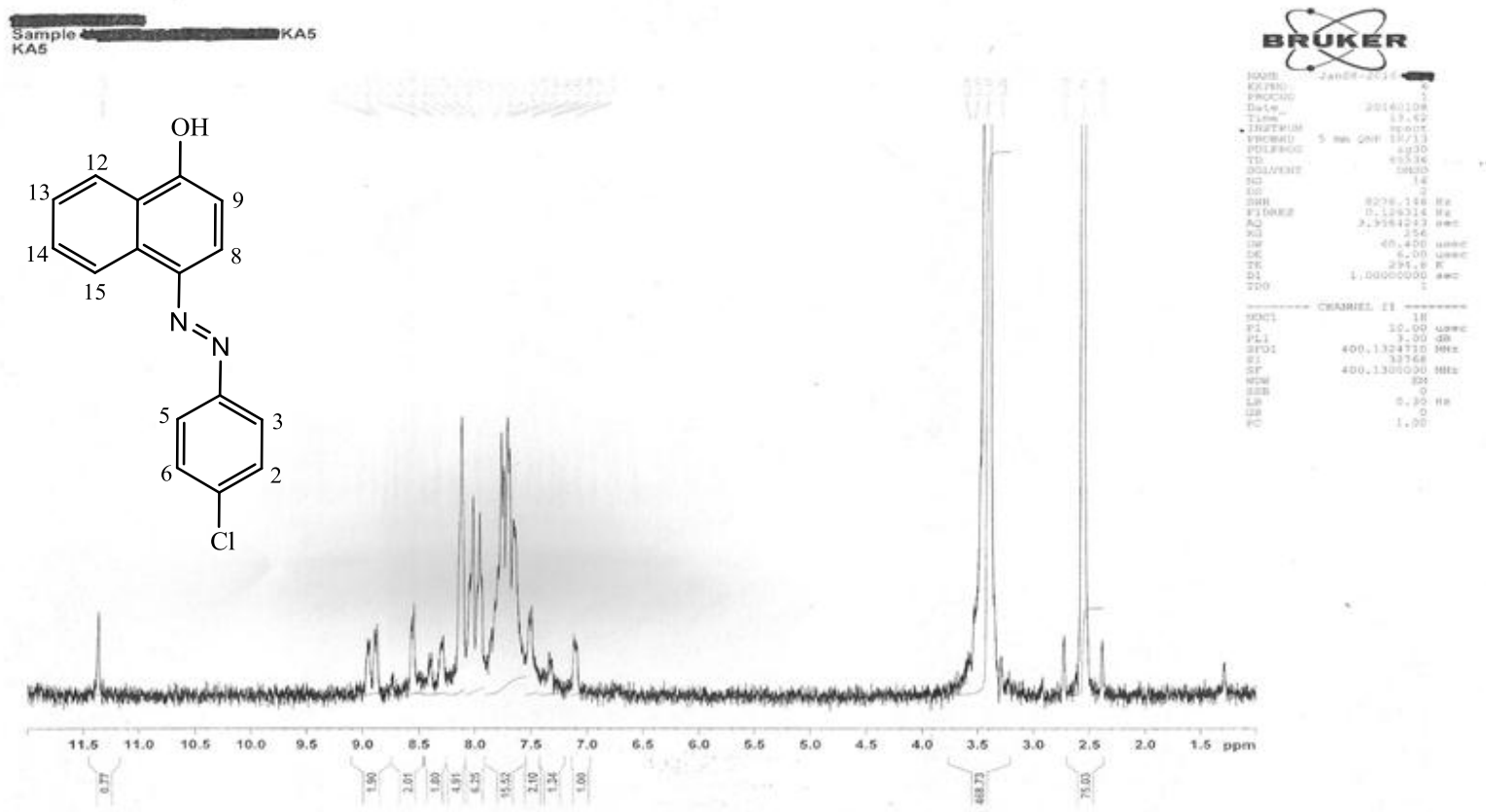
4: (Time: 3.40) Combine (91:95-(85:86+108:111)) 2:MS ES-
4.2e+006



6: (Time: 3.90) Combine (104:108-(99:101+113:116)) 2:MS ES-
1.4e+005



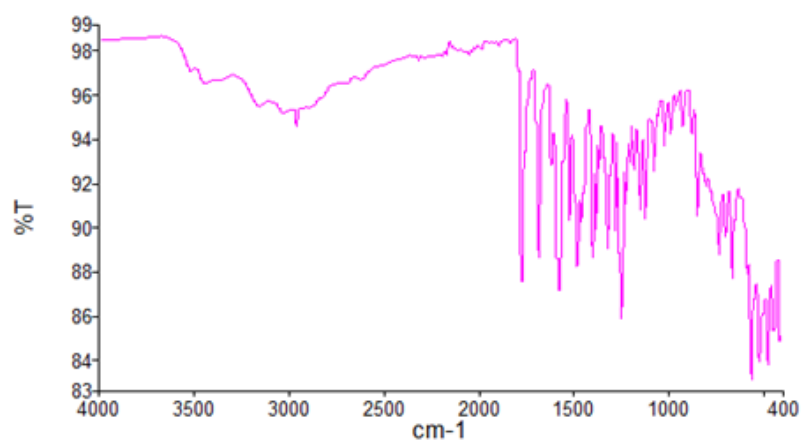
(3) ^1H NMR



Appendix F; Analytical Data for KA 006

(1) IR Spectrum

Spectrum Graph



| Name | Description |
|--------------------|-------------|
| Kwaku Addo-Danquah | KA 006 |

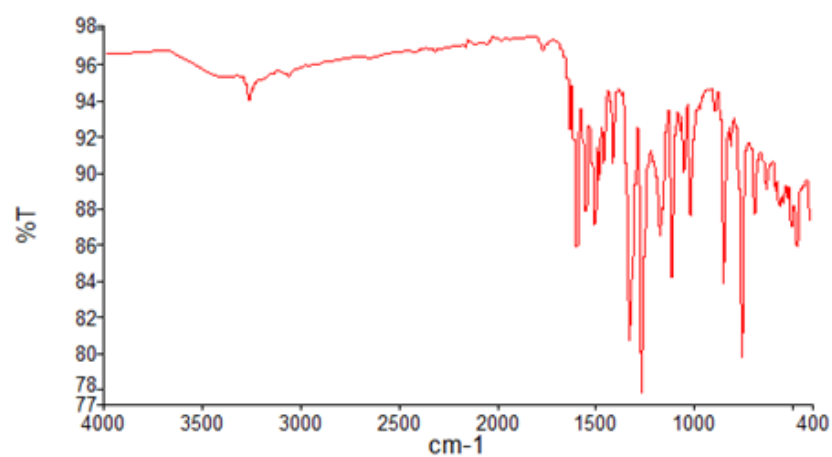
Peak Table

| Peak | X | Y |
|------|---------|-------|------|---------|-------|------|---------|-------|------|---------|-------|
| 1 | 2966.78 | 94.78 | 2 | 1772.65 | 87.53 | 3 | 1685.15 | 88.63 | 4 | 1577.14 | 87.17 |
| 5 | 1518.84 | 90.34 | 6 | 1481.54 | 88.22 | 7 | 1395.43 | 88.7 | 8 | 1378.23 | 89.95 |
| 9 | 1312.83 | 89.1 | 10 | 1281.89 | 89.91 | 11 | 1247.23 | 85.87 | 12 | 1143.7 | 90.85 |
| 13 | 1119.69 | 90.41 | 14 | 1075.97 | 92.66 | 15 | 1020.36 | 93.77 | 16 | 847.43 | 90.58 |
| 17 | 732.67 | 88.83 | 18 | 695.21 | 89.59 | 19 | 655.54 | 87.7 | 20 | 554.83 | 83.04 |
| 21 | 522.79 | 83.85 | 22 | 470.72 | 83.68 | 23 | 436.86 | 85.31 | | | |

Appendix G; Analytical Data for KA 007

(1) IR Spectrum

Spectrum Graph



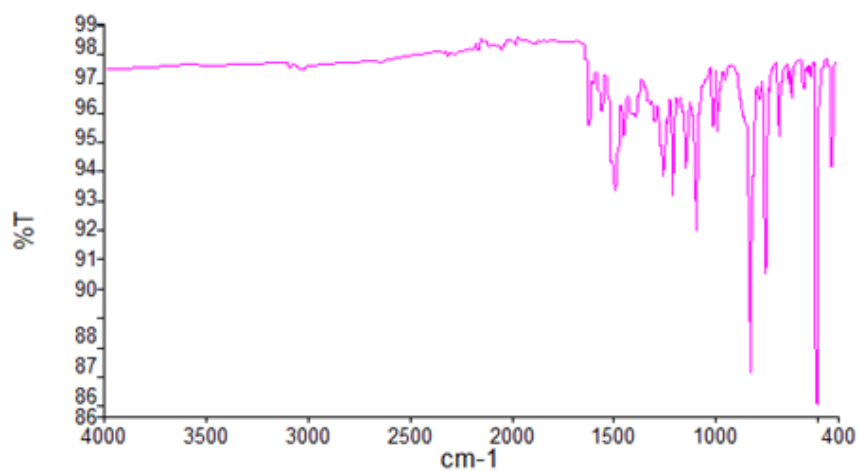
| Name | Description |
|--------------------|-------------|
| Kwaku Addo-Danquah | KA 007 |

Peak Table

| Peak | X | Y |
|------|---------|-------|------|---------|-------|------|---------|-------|------|---------|-------|
| 1 | 3287.51 | 94.19 | 2 | 1628.26 | 92.44 | 3 | 1594.61 | 85.86 | 4 | 1547.8 | 87.9 |
| 5 | 1502.56 | 87.14 | 6 | 1479.77 | 89.65 | 7 | 1457.81 | 90.58 | 8 | 1412.14 | 90.59 |
| 9 | 1320.05 | 80.67 | 10 | 1259.51 | 77.69 | 11 | 1167.67 | 86.55 | 12 | 1107.96 | 84.17 |
| 13 | 1047.12 | 90.04 | 14 | 1013.34 | 87.64 | 15 | 847.64 | 83.81 | 16 | 750.48 | 79.69 |
| 17 | 686.77 | 87.7 | 18 | 468.39 | 85.84 | | | | | | |

Appendix H; Analytical Data for KA 008

(1) IR Spectrum



| Name | Description |
|--------------------|-------------|
| Kwaku Addo-Danquah | KA 008 |

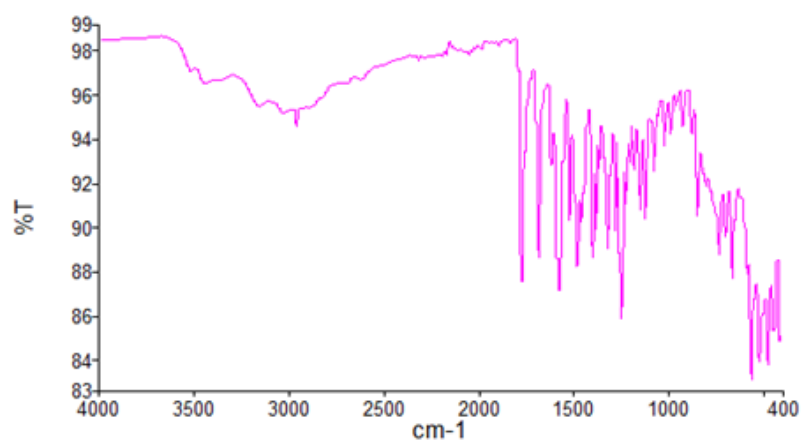
Peak Table

| Peak | X | Y |
|------|---------|-------|------|---------|-------|------|---------|-------|------|---------|-------|
| 1 | 1486.9 | 93.42 | 2 | 1254.26 | 93.9 | 3 | 1210.15 | 93.26 | 4 | 1147.19 | 94.19 |
| 5 | 1088.83 | 91.99 | 6 | 985.48 | 95.42 | 7 | 820.78 | 87.08 | 8 | 749.18 | 90.56 |
| 9 | 679.7 | 95.27 | 10 | 496.28 | 85.98 | 11 | 423.15 | 94.24 | | | |

Appendix I; Analytical Data for KA 009

(1) IR Spectrum

Spectrum Graph

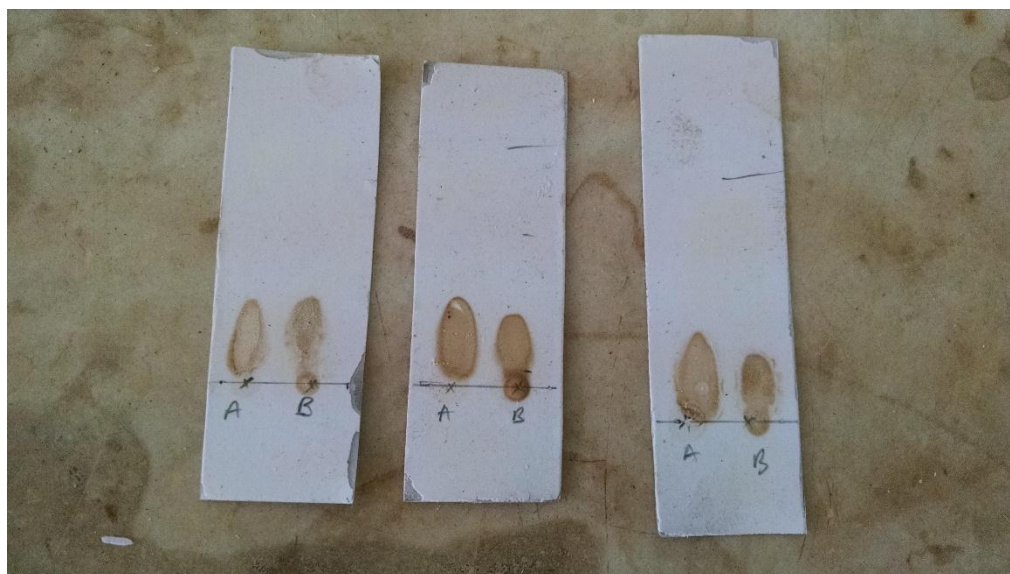


| Name | Description |
|--------------------|-------------|
| Kwaku Addo-Danquah | KA 006 |

Peak Table

| Peak | X | Y |
|------|---------|-------|------|---------|-------|------|---------|-------|------|---------|-------|
| 1 | 2966.78 | 94.78 | 2 | 1772.65 | 87.53 | 3 | 1685.15 | 88.63 | 4 | 1577.14 | 87.17 |
| 5 | 1518.84 | 90.34 | 6 | 1481.54 | 88.22 | 7 | 1395.43 | 88.7 | 8 | 1378.23 | 89.95 |
| 9 | 1312.83 | 89.1 | 10 | 1281.89 | 89.91 | 11 | 1247.23 | 85.87 | 12 | 1143.7 | 90.85 |
| 13 | 1119.69 | 90.41 | 14 | 1075.97 | 92.66 | 15 | 1020.36 | 93.77 | 16 | 847.43 | 90.58 |
| 17 | 732.67 | 88.83 | 18 | 695.21 | 89.59 | 19 | 655.54 | 87.7 | 20 | 554.83 | 83.04 |
| 21 | 522.79 | 83.85 | 22 | 470.72 | 83.68 | 23 | 436.86 | 85.31 | | | |

Appendix J: TLC profile for the alkylation using NaOH



A represents the spot for the starting material and B represents that of the reaction mixture. The TLC was developed after times, 0, 30 and 60 mins.